Chemical Geology 417 (2015) 44–57

Contents lists available at ScienceDirect

Chemical Geology

journal homepage: www.elsevier.com/locate/chemgeo

Standardless fission-track dating of the Durango apatite age standard

Raymond Jonckheere [a,b,*], Peter Van den haute [b], Lothar Ratschbacher [a]

[a] Geologisches Institut, Technische Universität Bergakademie Freiberg, Bernhard-von-Cottastraße 2, 09599 Freiberg (Sachsen), Germany
[b] Geologie en Bodemkunde, Universiteit Gent, Krijgslaan 281 (S8) 9000 Gent, Belgium

ARTICLE INFO

Article history:
Received 9 June 2015
Received in revised form 14 September 2015
Accepted 16 September 2015
Available online 28 September 2015

Keywords:
Durango apatite
Standardless fission-track dating
Plateau age
Length correction

ABSTRACT

Five dating strategies were used for determining the standardless fission-track age of the Durango apatite. These use the same fossil-track densities but differ in the manner in which the induced-track densities are determined. A conventional age calculation, without correction for experimental factors, gives inconsistent ages with method-related differences >15%. Correcting for these factors brings the ages in line with each other and with the reference age but leaves no room for a partial-annealing correction based on the confined-track lengths. Three further reasons suggest that a length correction is not appropriate. (1) The evidence for length-based corrections is inconclusive. (2) The plateau age of the Durango apatite is consistent with its apparent fission-track age to within 1%. (3) The calculated effective etchable length of the fossil tracks agrees within error with that of the induced tracks; both are further consistent with the measured mean length of confined induced tracks. The circumstance that the (U,Th)/He ages of the accepted and proposed apatite age standards are consistent with their reference ages leaves no margin for a lowered fission-track age resulting from partial annealing, although the case of the Durango apatite itself is inconclusive because of its exceptional crystal size. It is conjectured that the shortening of the fossil tacks in the Durango apatite is due to a lowering of the track etch rate over time. In this case, annealing equations fitted to induced-track data underestimate the extent of confined-track-length reduction in geological samples.

1. Introduction: premises

The progress of the fission-track dating method can be divided into a time before and an almost equal time since the recommendation of the ζ-calibration (Hurford, 1990a, b). During the first period, it was dogged by problems associated with the ^{238}U-fission constant, neutron-fluence measurement and experimental factors related to the dating techniques (Bigazzi, 1981). Since the acceptance of the ζ-calibration and the development of apatite (T,t)-path modelling (Crowley, 1985; Green et al., 1989), it has met with great practical success. A decade before the ζ-recommendation, Bigazzi (1981) proposed two strategies for overcoming the problems of the fission-track method. One comes down to what became the ζ-calibration. The other involves solving the methodological problems in three steps: (1) achieving accurate neutron-fluence measurements, (2) eliminating errors associated with the dating techniques, and (3) establishing a reliable correction for partial annealing of the fossil tracks. The question of the ^{238}U-fission constant would then resolve itself.

Our contribution sets out from the premise that neutron-fluence measurements using the recommended metal monitors (Au, Co) and well-thermalized irradiation facilities are no longer an issue (Bigazzi et al., 1990; Curvo et al., 2013; De Corte et al., 1991, 1995; Van den haute et al., 1988, 1998). Our second assumption is that the matter of the fission constant has been settled following recent redeterminations (Eikenberg et al., 1993; Guedes et al., 2000, 2003; Suzuki, 2005; Yoshioka et al., 2005) and reassessments (Holden, 1989; Holden and Hoffman, 2000). Our work concentrates instead on steps (2) and (3) of Bigazzi's (1981) research program by using five dating methods, requiring method-specific corrections for experimental factors, for determining the standardless fission-track age of the Durango apatite.

2. Adjusted age equation

Natural apatite contains trace amounts of uranium. A fraction of the isotope ^{238}U undergoes spontaneous fission over geological time. The nuclear fragments, moving in opposite directions through the lattice, produce a single ca. 20-μm long (Bhandari et al., 1971; Jonckheere, 2003a, b), <10-nm diameter (Afra et al., 2011; Jaskierowicz et al., 2004; Lang et al., 2015; Li et al., 2014; Miro et al., 2005; Paul and Fitzgerald, 1992; Schauries et al., 2014) fossil fission track. The number of tracks per unit volume (N_S) is proportional to the age (t) and ^{238}U content (U_{238}) of the sample and the spontaneous-fission rate (λ_F) of ^{238}U (Eq. 1).

$$N_S = \lambda_F \, t \, U_{238} \quad (1)$$

* Corresponding author at: Geologisches Institut, Technische Universität Bergakademie Freiberg, Bernhard-von-Cottastraße 2, 09599 Freiberg (Sachsen), Germany.
E-mail addresses: Raymond.Jonckheere@geo.tu-freiberg.de, Raymond.Jonckheere@Ugent.be (R. Jonckheere).

http://dx.doi.org/10.1016/j.chemgeo.2015.09.014
0009-2541/

Fission tracks also form when apatite is irradiated in a reactor. The thermal neutrons in the reactor spectrum cause a fraction of the ^{235}U isotope to fission, producing induced fission tracks. The number of induced tracks per unit volume (N_I) is proportional to the concentration of ^{235}U (U_{235}) and the fission rate $R_F = \sigma\phi$, wherein ϕ is the thermal-neutron fluence and σ the effective cross-section for ^{235}U-fission by thermal-neutron capture (Eq. 2).

$$N_I = \sigma\,\phi\,U_{235} \tag{2}$$

It follows from Eqs. (1) and (2) that:

$$t = (\lambda_F)^{-1}\,(N_S/N_I)\,(U_{235}/U_{238})\,\sigma\,\phi \tag{3}$$

Eq. (1) neglects the depletion of ^{238}U by spontaneous fission and α-disintegration. An exact equation derived by Price and Walker (1963) implies that Eq. (1) is accurate to within 1% for $t < 10^{10}$ a. Eq. (2) does not account for burn-up of ^{235}U or for the production of induced tracks by epithermal- and fast-neutron fission of ^{235}U. Eqs. (1) and (2) furthermore do not consider spontaneous or induced fission of other isotopes. In practice, these are negligible for the neutron fluences required for dating apatite and for irradiations in well-thermalized reactor channels (Tagami and Nishimura, 1992; Wagner and Van den haute, 1992). Eq. (3) is adequate for dating samples up to 100 Ma.

There is a complication related to the ^{235}U-fission rate $R_F = \sigma\phi$ in Eq. (3), when ϕ is calculated from the γ-activities of co-irradiated metal-activation monitors (Au, Co). This calculation is in practice based on the "simple" Høgdahl formalism, which can cope with non-ideal epithermal-neutron spectra, and gives the conventional sub-cadmium neutron fluence ϕ_S. The Høgdahl formalism is however not suited for non-(1/v) reactions such as thermal-neutron induced ^{235}U fission. The appropriate formalism for non-(1/v) reactions is the more sophisticated Westcott convention, which includes the $g(T_n)$ correction factor (Westcott g-factor; T_n: Maxwellian neutron temperature) and uses the conventional total (Westcott) neutron fluence ϕ_W. It can be shown that in well-thermalized irradiation channels $\phi_W \approx \phi_S$ ($\phi_W = \beta\,\phi_S$). In channel 8 of the Thetis nuclear reactor (Universiteit Gent; thermal to epithermal fluence ratio: $f = 155$; epithermal spectrum parameter: $\alpha = 0.10$), used for the irradiations in this work, $\beta = 1.0025$ (Jonckheere, 1995; Verheijke, 1994) and $g(T_n) = 0.9832$ (Holden, 1999; $T_n = 27$ °C: Wagemans et al., 1988). Another consideration concerns the rare-earth-element content of the Durango apatite, in particular the Gd concentration of up to 200 ppm. Its high neutron-absorption cross-section (ca. 49,000 b) can cause fluence depression in the samples of up to ca. 4% (Naeser and Fleischer, 1975). The calculated correction factor for thermal-neutron shielding (G_{th}; De Corte et al., 1991) in the Durango sections dated here is $G_{th} = 0.986 \pm 0.001$ (Bellemans, pers. com.; Jonckheere, 2003b). Combining these factors, the fission rate $R_F = \sigma\phi$ in Eq. (3) can be rewritten as:

$$R_F = (g(T_n)\,\sigma_0)\,(G_{th}\,\beta\,\phi_S) = 0.972\,(\sigma_0\,\phi_S). \tag{4}$$

σ_0 is the conventional (2200 m/s) fission cross-section of ^{235}U ($\sigma_0 = 586 \pm 3$ b; Holden and Holden, 1989) and ϕ_S the conventional subcadmium neutron fluence calculated from the measured γ-activities of the co-irradiated metal-activation monitors using the Høgdahl formalism.

The natural isotopic ratio $I = \theta_{235}/\theta_{238}$ ($7.253\ 10^{-3}$; Cowan and Adler, 1976) is substituted for (U_{235}/U_{238}) in Eq. (3) for calculating the age of a sample. This is accurate if U_{238} and U_{235} in Eqs. (1)–(3) refer to the same elemental uranium concentration, i.e. if the fossil and induced fission-track densities, N_S and N_I, have been produced by the same concentration of uranium atoms. Natural apatite minerals often exhibit within-grain and between-grain uranium inhomogeneities. For this reason, the estimates of N_S and N_I are either each averaged over representative grain samples (multi-grain or population methods) or both measured in the same grains (single-grain or matched-areas methods; Gleadow, 1981; Galbraith, 1981).

The external-detector method (Gleadow, 1981) is the single-grain method most used for dating. The fossil tracks are counted in a polished internal apatite surface and the induced tracks in an external detector irradiated in contact with it. Thus, the fossil tracks result from uranium fission on both sides of the etched apatite surface (4π-geometry) whereas the induced tracks result from uranium fission on one side of the surface of the external detector (2π-geometry). The ratio of the fossil to induced-track densities (ρ_S/ρ_I) is therefore multiplied by a geometry factor G ($= 2\pi/4\pi$). This also applies to the re-etch method (Gleadow, 1981), where the induced tracks are counted in an external apatite surface.

The Durango apatite dated in this work consists of cm-sized crystals, which were cut into ca. ½-mm thick sections for the specific purpose of comparing the fission-track ages of basal and prism faces. Part of the analyses was carried out with a population method. In our case this did not involve different aliquots but different sections from a single crystal (Section 3). One section was annealed and irradiated for counting the induced tracks, while the adjoining section, which was neither annealed nor irradiated, was used for counting the fossil tracks. In the presence of uranium-concentration gradients, this presents a risk of systematic error. To avoid it, both sections were re-irradiated in contact with muscovite external detectors. A correction factor U can then be calculated from the induced-track densities ρ_{ED} in both external detectors and the respective neutron fluences ϕ_S:

$$U = (\rho_{ED}/\phi_S)_I/(\rho_{ED}/\phi_S)_S. \tag{5}$$

The subscripts outside the brackets refer to the irradiations of the sections with fossil (S) and induced (I) tracks. The single-grain dating methods present a similar problem. For the external-detector and re-etch methods (Gleadow, 1981), it is assumed that half the uranium that produced the fossil tracks is not available for producing induced tracks during neutron irradiation. In the presence of significant short-range uranium variation perpendicular to the apatite surface, this assumption is invalid. We have no means of accounting for it, and assume that it is negligible ($U = 1$). With the repolish method (Gleadow, 1981), there is a small offset between the sections used for counting the fossil and induced tracks due to the intervening repolish. It is again assumed that no correction is required.

N_S and N_I in Eq. (3) are volumetric track densities. In practice, the fossil and induced tracks intersecting the detector surface are enlarged by etching and their areal densities (ρ_S and ρ_I) are determined by counting under a microscope. Because of etching and observation effects, the track-counting efficiencies $[\eta q]_S$ and $[\eta q]_I$ (Jonckheere, 1995, 2003b; Wagner and Van den haute, 1992) are in general <1. For dating methods where ρ_S and ρ_I are determined in different track-registration geometries, it cannot be assumed that $[\eta q]_S = [\eta q]_I$ (Jonckheere and Van den haute, 1998, 1999, 2002). This is accounted for by introducing a procedure factor $Q = [\eta q]_I/[\eta q]_S$ and substituting $(N_S/N_I) = Q\,(\rho_S/\rho_I)$ in Eq. (3).

It is expedient to introduce an etch-time factor T for the re-etch method (Gleadow, 1981), in which the fossil tracks are etched before ($\rho_S(t_E)$; t_E: etch time) and after irradiation ($\rho_S(2t_E) + \rho_I(t_E)$). Because of the etch-time difference, it should not be assumed that the fossil tracks are revealed and identified the same in both counts ($[\eta q]_S(2t_E) \neq [\eta q]_S(t_E)$ or $\rho_S(2t_E) \neq \rho_S(t_E)$). T can be determined from step-etch experiments ($T = \rho_S(t_E)/\rho_S(2t_E)$). T is important for correcting for the effect of residual etch figures, i.e. etch pits that persist after the lower track end-points have been overtaken by surface etching (Jonckheere and Van den haute, 1996).

A fission fragment crossing from mineral to external detector leaves a damage trail in both. However, not every etched track in the mineral corresponds to one in the external detector (Iwano and Danhara,

1998; Iwano et al., 1992, 1993; Jonckheere, 1995, 2003b) due to their different track-revelation thresholds (range deficits; Fleischer et al., 1975). A fraction of the fission fragments crossing the contact between an apatite sample and a muscovite external detector leaves an etchable track in the mica but not in the apatite (Jonckheere, 2003b). This requires an additional correction factor R ($= 1.21 \pm 0.03$; range deficit factor) in Eq. (3).

The number of etched tracks intersecting a unit surface (ρ) is a function of their etchable length (l; Fleischer et al., 1975). Due to geological annealing, the etchable lengths of fossil tracks (l_S) in natural apatites are shorter than those of induced tracks (l_I). A correction factor L can be included in Eq. (3) for dating the onset of track retention, i.e. for calculating the age of the oldest surviving track, allowing for subsequent partial annealing. The relationship between the mean length (l/l_0) and density (ρ/ρ_0) of induced tracks has been investigated in annealing experiments (Green, 1988; Laslett et al., 1984; Naeser et al., 1989; Watt and Durrani, 1985; Watt et al., 1984). The equations fitted to the data (Crowley, 1993; Guedes et al., 2004; Ketcham, 2005; Ketcham et al., 2000; Lutz and Omar, 1991; Naeser et al., 1989; Tello et al., 2006; Willett, 1997) agree on an approximate 1:1 relationship between (ρ/ρ_0) and (l/l_0) down to $l/l_0 \leq 0.7$. The fossil tracks in the Durango apatite are ca. 10% shorter than the induced tracks (Gleadow et al., 1986; Green, 1988; Green et al., 1986). The length-correction factor is thus given by: $L \approx l_I/l_S$, although its exact value would be slightly higher due to the broadening of the fossil-track-length distribution, and somewhat dependent on the annealing equations and (T,t)-history (Wauschkuhn et al., 2015a).

The lengths used for age correction are those of the fossil (l_S) and induced (l_I) confined tracks. However, with the aid of the track-counting efficiencies (ηq) and known physical constants, it is possible to calculate the effective lengths of the fossil ($l_{S,0}$) and induced ($l_{I,0}$) tracks from the corresponding track densities (ρ_S, ρ_I). This requires a known reference age, an independent estimate of its uranium concentration, and that the thermal-neutron fluence has been measured with metal-activation monitors. The equations for calculating the uranium content from the track densities (ρ_{ED}) in co-irradiated external detectors (Enkelmann et al., 2005a; Hoffmann et al., 2008), the standardless fission-track ages (ϕ-ages; Jonckheere, 2003b) and the effective length of the fossil and induced tracks (Jonckheere, 1995) are summarized in Table 1, with the requisite numerical values.

3. Samples and experiments

The experiment was carried out on the Durango apatite from the Oligocene Cerro de Mercado iron-ore deposit (Durango, Mexico), where it occurs in association with martite within a volcanic series (Alva-Valdivia et al., 2001; Corona-Esquivel et al., 2007, 2009; Foshag, 1929; Lyons, 1988; McDowell et al., 2005; McDowell and Keizer, 1977; Swanson et al., 1978). The distinctive cm-sized transparent yellow crystals contain inclusions and exhibit chemical zonation (Hasebe et al., 2013; Johnstone et al., 2013; Marks et al., 2012; Pellas and Perron, 1984). Its crystal properties ($a = b = 9.3955$ Å; $c = 6.8801$ Å; Stock et al., 2015; Young et al., 1969) and chemical composition are well established, with substantial substitutions of LREE at the $Ca^{2+}(2)$-site and HREE at the $Ca^{2+}(1)$-site, charge balanced by Na^{+}/Ca^{2+} and Si^{4+}/P^{5+} substitutions (Rønsbo, 1989) and a F:Cl-ratio of ca. 8:1. (Barbarand and Pagel, 2001a, b; Barbarand et al., 2003a; Belousova et al., 2002; Carlson et al., 1999; Goldoff et al., 2012; Marks et al., 2012; McCubbin et al., 2010; Morishita et al., 2008; Patiño Douce et al., 2011; Roeder et al., 1987; Rogers et al., 1984; Teiber et al., 2015; Yang et al., 2014; Young et al., 1969). The actinide concentrations are ca. 7–22 ppm U and 150–380 ppm Th (Abdullin et al., 2014; Boyce and Hodges, 2005; Chew et al., 2014; Johnstone et al., 2013; Kimura et al., 2000; Morishita et al., 2008; Soares et al., 2014; Young et al., 1969).

Table 2 summarizes some geochronological data relating to the Durango apatite; classical fission-track ages are not included. The Fission Track Working Group of the I.U.G.S. Subcommission on Geochronology recommended the Durango apatite as one of two apatite age standards for fission-track dating (Hurford 1990a, b). It has since also been adopted as an age-reference material for apatite (U,Th)/He dating and for other dating methods as well. Although the reference age of the Durango apatite is not specified in the recommendation, it is understood that the recommended value is that based on the K/Ar ages of ignimbrites bracketing the Mercado Iron Member, determined by F.W. McDowell (McDowell and Keizer, 1977), reported by Naeser and Fleischer (1975) and recalculated by Green (1985) with the constants

Table 1
Equations, physical constants and numerical values for calculating the uranium concentrations, the fission-track ages and plateau age of the Durango apatite and the effective lengths of the fossil and induced tracks. Reactor-specific values refer to channel 8 of the Thetis reactor (Universiteit Gent). Values specific to the track counts and length measurements refer to the etching conditions in this work. Errors are 1σ.

Equation	Factor	Value	Reference
(6) Uranium concentration:	d_A	3.2 ± 0.1 g cm^{-3}	McConnel (1973)
$[U]\ (\text{ppm}) = \left[\frac{2\ A_U [2R]_M 10^6}{g_{ED}\ [\eta q]_{ED} [2R]_A\ l_M\ G_{th}\ g(T_n)\ \beta\ \sigma_0\ \theta_{235}\ d_A\ N_A}\right] \frac{\rho_{ED}}{\phi_S}$	N_A	$6.022\ 10^{23}$	Avogadro's number
	A_U	238.08	mass uranium atom
	θ_{235}	0.00720	Steiger and Jäger (1977)
$= (6.73 \pm 0.19) 10^{10}\ \frac{\rho_{ED}}{\phi_S}$	I	$7.253\ 10^{-3}$	Cowan and Adler (1976)
(7) FT age (no subtraction):	λ_α	$(1.551 \pm 0.007)\ 10^{-10}$ a^{-1}	Jaffey et al. (1971); Holden (1989)
$t_A = \left(\frac{1}{\lambda_\alpha}\right) , \ln\left[\left(\frac{\lambda_\alpha}{\lambda_F}\right) G\ Q\ R\ U \left(\frac{\rho_S}{\rho_I}\right) I\ (g(T_n)\ \sigma_0)\ (G_{th}\ \beta\ \phi_S) + 1\right]$	λ_F	$(8.45 \pm 0.10)\ 10^{-17}$ a^{-1}	Holden and Hoffman (2000)
	σ_0	586 ± 3 barn	Holden and Holden (1989)
(8) FT age (w. subtraction):	$g(T_n)$	0.9832	Holden (1999)
$t_A = \left(\frac{1}{\lambda_\alpha}\right) , \ln\left[\left(\frac{\lambda_\alpha}{\lambda_F}\right) G\ Q\ R\ U \left(\frac{\rho_S}{\rho_{I+S} - T\ \rho_S}\right) I\ (g(T_n)\ \sigma_0)\ (G_{th}\ \beta\ \phi_S) + 1\right]$	G_{th}	0.986 ± 0.001	Bellemans (pers. com.)
	β	1.0025	Jonckheere (1995)
	G, g_{IS}, g_{ED}	½ or 1	Gleadow (1981); Jonckheere (2003b)
	$Q = [\eta q]_{IS/ES/ED}/[\eta q]_{IS}$		Method-dependent procedure factor
(9) Length of induced tracks:	$[\eta q]_{IS}$	0.91 ± 0.01	Jonckheere and Van den haute (2002)
$l_{I,0}\ (\mu\text{m}) = \left[\frac{2\ A_U\ 10^6}{g_{IS} [\eta q]_{IS}\ G_{th}\ g(T_n)\ \beta\ \sigma_0\ \theta_{235}\ d_A\ N_A}\right] \frac{\rho_I}{\phi_S\ [U](\text{ppm})}$	$[\eta q]_{ES}$	1.01 ± 0.01	Jonckheere and Van den haute (2002)
	$[\eta q]_{ED}$	0.91 ± 0.01	Jonckheere and Van den haute (2002)
	$[2R]_A/[2R]_M$	0.962 ± 0.017	Jonckheere (2003b)
$= (6.63 \pm 0.13) 10^7\ \frac{\rho_I}{\phi_S\ [U](\text{ppm})}$	R	1.21 ± 0.03	Jonckheere (2003b)
(10) Length of fossil tracks:	U	Table 3	Enkelmann et al. (2005a)
$l_{S,0}\ (\mu\text{m}) = \left[\frac{2\ \lambda_\alpha\ A_U\ 10^6}{g_{IS} [\eta q]_{IS}\ \lambda_F\ \theta_{238}\ d_A\ N_A\ [e^{(\lambda_\alpha t_R} - 1]}\right] \frac{\rho_S}{[U]\ (\text{ppm})}$	T	Table 5	Jonckheere and Van den haute (1996)
	l_S	14.5 ± 0.1 μm	Jonckheere and Van den haute (2002)
	l_I	16.3 ± 0.1 μm	Jonckheere and Van den haute (2002)
$= (1.03 \pm 0.02) 10^{-7}\ \frac{\rho_S}{[U]\ (\text{ppm})}$	l_M	20.5 ± 0.3 μm	Bigazzi (1967); Nagpaul et al. (1974); Guedes et al. (2008)
	t_R	31.4 ± 0.3 Ma	McDowell and Keizer (1977); Green (1985)

Table 2
Published geochronological and induced and fossil track-length data for the Durango apatite. *N*: number of measurements; method: decay process on which the age determination is based; (U,Th)/He does not mean that Sm is not considered (see references for methodological details); t_E (s): etching time; C_E (M HNO_3): etchant concentration; T_E (°C): etchant temperature; RT: room temperature; [1] ^{207}Pb-corrected ^{238}U/^{206}Pb-age; [2] uncorrected ^{232}Th/^{208}Pb-age; [3] Concordia age (65 μm spot); [4] Concordia age (110 μm spot); [5] ^{207}Pb-corrected mean age; [6] ^{204}Pb-corrected Concordia age; [7] calculated with (U,Th)-concentrations from Zeitler et al. (1987); [8] calculated with (U,Th)-concentrations from Young et al. (1969) and Naeser and Fleischer (1975); [9] laser degassing; [10] furnace degassing; [11] Durango apatite uranium standard; [12] Mud Tank apatite uranium standard; [13] number of dated units; [14] tracks etched 10 min after irradiation; [15] tracks etched 41 days after irradiation. Errors recalculated to 1σ.

Age (Ma)	*N*	Method	Reference
Individual measurements			
30.6 ± 1.2[1]|32.5 ± 0.6[2]	19|19	U/Pb|Th/Pb	Chew et al. (2011)
33.0 ± 1.2	45	U/Pb	Chew and Donelick (2012)
31 ± 2	18	U/Pb	Li et al. (2012)
32.2 ± 2.7[3]|32.0 ± 1.5[4]	10|5	U/Pb	Thomson et al. (2012)
32.0 ± 0.3[5]|31.8 ± 0.2[6]	36|36	U/Pb	Chew et al. (2014)
31.1 ± 0.3	12	U/Pb	Cochrane et al. (2014)
31.4 ± 0.3	14	K/Ar	McDowell and Keizer (1977); Green (1985)
31.4 ± 0.1	4[13]	Ar/Ar	McDowell et al. (2005)
43.2[7]| 32.2[8]	1	(U,Th)/He	Zeitler et al. (1987)
33.9	1	(U,Th)/He	Wolf et al. (1996)
27.5 ± 1.5	1	(U,Th)/He	Warnock et al. (1997)
32.3 ± 0.2	25	(U,Th)/He	House et al. (1999)
32.1 ± 1.7[9]|32.1 ± 1.7[10]	11|16	(U,Th)/He	House et al. (2000)
31.0 ± 0.2	24	(U,Th)/He	McDowell et al. (2005)
31.4 ± 0.3	34	(U,Th)/He	Solé and Pi (2005)
32.8 ± 1.8	11	(U,Th)/He	Foeken et al. (2006)
30.9 ± 0.9	17	(U,Th)/He	Spiegel et al. (2009)
34.1 ± 0.6	5	(U,Th)/He	Gong et al. (2013)
32.2 ± 1.0	15	(U,Th)/He	Johnstone et al. (2013)
30.5 ± 2.2	–	(U,Th)/He	Mahéo et al. (2013)
31.0 ± 0.3	61	(U,Th)/He	Shan et al. (2013)
30.6 ± 0.7	3	(U,Th)/He	Zeng et al. (2013)
32.6 ± 1.5	6	(U,Th)/He	Legrain et al. (2014)
32.6 ± 0.7	3	(U,Th)/He	Cox et al. (2015)
33.7 ± 1.8	9	(U,Th)/He	Hoke et al. (2015)
31.7 ± 9.4	2	(U,Th)/Ne	Gautheron et al. (2006)
34.5 ± 3.3	9	(U,Th)/Ne	Cox et al. (2015)
34.2 ± 8.6	1	(U,Th)/(Ne,He)	Gautheron et al. (2006)
29.7 ± 1.9	1	FT ICP-MS	Hasebe et al. (2004)
31.2 ± 0.2	104	FT ICP-MS	Abdullin et al. (2014)
31.4 ± 2.5[11]|31.8 ± 2.4[12]	1|1	FT ICP-MS	Soares et al. (2014)
Lab averages			
32.1|32.0	>30	(U,Th)/He	Caltech (Farley, 2000, 2002)
31.0 ± 0.9	70	(U,Th)/He	CSIRO (Evans et al., 2005)
31.9 ± 0.1	169	(U,Th)/He	Arizona (Reiners and Nicolescu, 2006)
32.1 ± 1.1	156	(U,Th)/He	Yale (Min et al., 2006)
31.7 ± 0.3	59	(U,Th)/He	Tübingen (Danišík et al., 2008)
31.1 ± 0.9	23	(U,Th)/He	Curtin (Danišík et al., 2012)
30.8 ± 1.4	38	(U,Th)/He	Waikato (Piotraschke et al., 2015)

Track length (μm)	t_E (s)	C_E (M)	T_E (°C)	Reference
Induced tracks				
15.2 ± 0.1	180	0.8	RT	Green (1981)
15.0 ± 0.1–15.2 ± 0.2	45	0.8	RT	Watt et al. (1984)
15.2 ± 0.1–17.1 ± 0.1	45–180	0.8	RT	Watt and Durrani (1985)
15.9 ± 0.1–16.5 ± 0.1	20	5.0	20	Gleadow et al. (1986); Green et al. (1986)
15.9 ± 0.1	20	5.0	20	Green (1988)
16.2 ± 0.1–16.6 ± 0.1[14]	25	5.0	23	Donelick et al. (1990)
16.2 ± 0.1–16.3 ± 0.1[15]	25	5.0	23	Donelick et al. (1990)
16.2 ± 0.1–17.5 ± 0.1	15–60	5.5	21	Carlson et al. (1999)
15.3 ± 0.8	55	0.8	22	Barbarand and Pagel (2001b)
16.3 ± 0.2	50	0.8	20	Iunes et al. (2002)
16.3 ± 0.1	60	0.4	25	Jonckheere and Van den haute (2002)
15.8 ± 0.1–16.1 ± 0.1	20	5.0	20	Barbarand et al. (2003b)
15.8 ± 0.1–16.0 ± 0.1	20	5.0	20	Barbarand et al. (2003a)
17.0 ± 0.1–17.3 ± 0.1	47	5.0	20	Ravenhurst et al. (2003)
16.1 ± 0.1–16.3 ± 0.1	50	1.3	20	Tello et al. (2006)
16.1 ± 0.1–16.2 ± 0.1	20–40	5.5	21	Jonckheere et al. (2007)
16.2 ± 0.1–16.4 ± 0.1	15–35	4.0	25	Jonckheere et al. (2007)
16.2 ± 0.1–16.5 ± 0.1	20	5.5	21	Chew and Donelick (2012)
15.8 ± 0.1	20	5.0	20	Schmidt et al. (2014)
Fossil tracks				
14.1 ± 0.1–14.8 ± 0.1	20	5.0	20	Gleadow et al. (1986)
14.2 ± 0.1	20	5.0	20	Green (1988)
14.9 ± 0.1	65	0.4	25	Jonckheere et al. (1993)
13.9 ± 0.2–14.9 ± 0.2	50	0.8	20	Iunes et al. (2002)

(continued on next page)

Table 2 (*continued*)

Track length (μm)	t_E (s)	C_E (M)	T_E (°C)	Reference
14.5 ± 0.1	60	0.4	25	Jonckheere and Van den haute (2002)
Fossil tracks				
14.3 ± 0.1	70	0.4	25	Enkelmann and Jonckheere (2003)
14.3 ± 0.1	20	5.5	21	Enkelmann and Jonckheere (2003)
13.7 ± 0.1–14.7 ± 0.1	20	4.0	25	Jonckheere et al. (2007)

recommended by Steiger and Jäger (1977): 31.4 ± 0.5 Ma (2σ; comment (5) to Tables 2 in Hurford, 1990a, b). This value was confirmed and specified by Ar/Ar dating of the same units: 31.4 ± 0.2 Ma (2σ; McDowell et al., 2005). The other radiometric ages in Table 2 have been determined on the Durango apatite itself, but are less precise or have been obtained with methods susceptible to methodological issues (low age; low U content; high Th/U-ratio; radiation damage effects) that have only begun to be addressed, or both. The recommended reference age is therefore adopted here: 31.4 ± 0.5 Ma (2σ).

Sixteen sections were cut from four Durango apatite crystals with a Struers Accutom 50 instrument, four from each crystal. Two crystals were cut perpendicular to the *c*-axis, giving eight basal sections; the two remaining crystals were cut parallel to the *c*-axis, giving eight prism sections. Four basal sections and four prism sections were annealed for 10 h at 450 °C to erase the fossil tracks, and mounted in resin. After curing for 24 h at 45 °C, the mounts were ground and polished with 6-μm, 3-μm and 1-μm diamond pastes on a Struers DPU-4 apparatus. The thickness of the mounts was reduced to 2 mm before irradiation. A 1-cm^2 muscovite external detector was attached to each mount. The samples were stacked in an irradiation can, together with Au, Co and Cu monitors for determining the thermal-neutron fluence (Au, Co) and axial and radial fluence gradients (Cu), and irradiated in channel 8 of the Thetis-reactor of the Universiteit Gent. All but one basal and one prism section with induced tracks were again cut out of the resin after the irradiation (Fig. 1).

Each section was paired with one which had adjoined it in the crystal and that had not been annealed or irradiated. Four sets were assembled; each set comprised a pair of basal sections and a pair of prism sections. Each such pair consisted of a section with fossil tracks and one with induced tracks. One set was annealed for 1 h at 250 °C in a Naber N3 muffle oven, another set at 300 °C and a third at 350 °C; the fourth set was not annealed. The purpose of these annealing steps was to determine the plateau age of the Durango apatite. Because of a transient 5 °C temperature drop following insertion of the samples in the oven and 5 °C oscillations during the experiment, the cited temperatures are nominal. This has no consequences for the plateau age because the pairs of sections with fossil and induced tracks were annealed in close contact. The basal and prism sections with induced tracks of the unannealed set had been polished before irradiation and not unmounted or repolished after. The induced tracks were thus registered in external apatite surfaces (2π) while the fossil tracks in the corresponding unirradiated sections were registered in internal surfaces. This made it possible to date the Durango apatite with a variant of the population method, not used for dating applications (method B). It has methodological interest, however, because, in contrast to the familiar population method (method A), it involves a geometry factor of ½ and ηq-factor for induced-track counts in an external apatite surface, $[\eta q]_{ES}$, resulting in a *Q*-factor like that for the re-etch method (method D).

The fourteen unmounted apatite sections were thereupon mounted in resin, ground and polished as before. All apatite sections were etched for 60 s in 2.5% HNO_3 at 25.0 ± 0.1 °C in a forced-circulation thermostatic bath. The etchant temperature was recorded with a Julabo TD-300 digital thermometer with a Pt-100 sensor. After etching and rinsing in p.a. ethanol, the eight sections with fossil tracks were covered with 1-cm^2 muscovite external detectors, stacked in an irradiation can with Au, Co and Cu monitors for measuring the thermal-neutron fluence (Au, Co) and axial and radial fluence gradients (Cu), and irradiated in channel 8 of the Thetis reactor. After irradiation, the external detectors were detached and etched, together with those from the first irradiation, for 20 min in 40% HF at 25.0 ± 0.1 °C.

At this stage, there were sixteen etched apatite sections and their corresponding external detectors (Fig. 1). Four apatite sections, the basal and

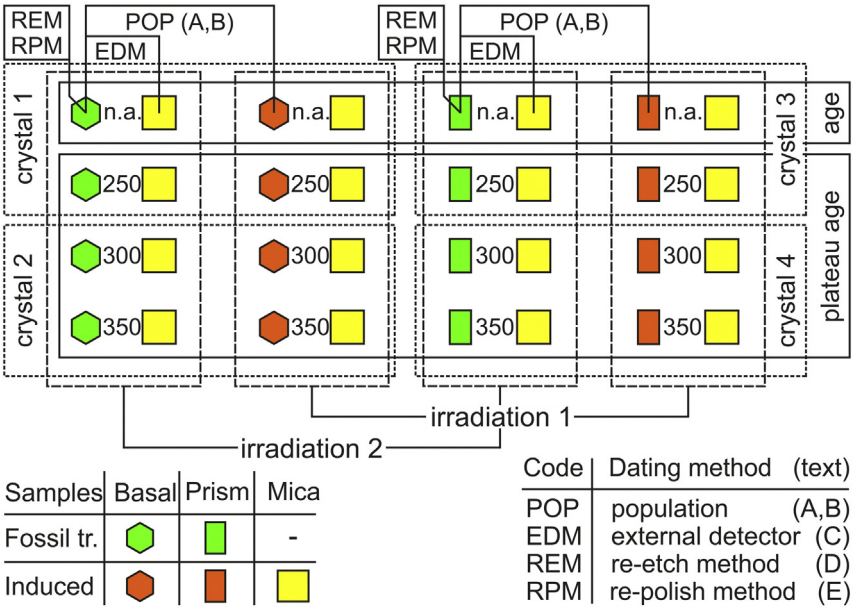

Fig. 1. Schematic organization of the experiment, showing the 8 basal and 8 prism sections of Durango apatite and their external detectors, the two irradiations, and the samples used for dating with different methods and for the determination of the plateau age. See text for details.

prism sections with fossil tracks and those with induced tracks that had not been annealed after the first irradiation were used for the age determinations. The remaining twelve sections that had been partially annealed, i.e. a pair of basal sections and a pair of prism sections annealed for 1 h at 250 °C and the corresponding pairs annealed at 300 °C and 350 °C were used for determining the plateau age. The external-detector counts were used for calculating the uranium content of all sections.

The weights of the co-irradiated metal-activation monitors were measured on electronic and mechanical scales to a precision of 0.01%; the maximum deviation between the instruments was <0.1%. The γ-activities were measured on a single-open-ended Ge(Li) detector linked to a Canberra-S40 4000-channel analyser. The wireform monitors were wound into tight spirals with approximate point source geometries and measured at the reference distance of 15 cm, for which a peak-detection-efficiency calibration curve (log ε_P vs. log E_γ) had been established by reactor staff with the aid of calibrated point sources. The measurements were continued until >50,000 counts had been collected under each peak. Accidental and true-coincidence losses are negligible for the source-detector distance and low count rates of the measurements (Moens, 1981). The peak areas were calculated assuming a sigmoidal background for the 411.8 keV ^{198}Au γ-peak and the 1173.2 keV and 1332.5 keV ^{60}Co γ-peaks (Sequal program; Op de Beeck, 1976) and a trapezoidal background for the 511.0 keV ^{64}Cu annihilation peak (Trap program). The fluence calculations were carried out in the Høgdahl convention using the formulae and nuclear constants in Van den haute et al. (1988) and De Corte et al. (1991). The unweighted mean of the fluences calculated from the 1173.2 keV and 1332.5 keV ^{60}Co γ-peaks was taken as the final Co-fluence, and averaged with the value calculated from the 411.8 keV ^{198}Au γ-peak to obtain the final estimate of the sub-cadmium neutron fluence in the Høgdahl formalism (ϕ_S). Fluence gradients were calculated from the 511.0 keV activities of the Cu monitors (Van den haute and Chambaudet, 1990) and assumed linear over the dimensions of the sample stack. The fluence for each sample was calculated by interpolation.

The track counts in apatite were carried out in transmitted light with an Olympus BH-2 microscope, equipped with a dry no-cover 100× objective and 10× eye pieces. The nominal magnification, including a drawing tube factor (1.25×), was 1250×. The size of the 10 × 10 counting grid was calibrated with a Graticules (50 × 2)-μm stage micrometre and amounted to 78.5 μm × 78.5 μm (6.16 10^{-5} cm^2); the actual overall magnification was 1274×. The track counts in the external detectors were carried out with cover glass and a 100× oil-immersion objective and 10× eye pieces. The size of the counting grid was 82.9 μm ×82.9 μm (6.87 10^{-5} cm^2) and the actual magnification 1206×. The cover glass served to protect the mica, which is more easily scratched and more difficult to clean than the apatite mounts.

These and the following experimental steps had four goals: (1) ascertaining the uranium concentration of the apatite sections; (2) dating basal and prism sections of the Durango apatite with the population method (A), a variant of the population method (B), the external-detector method (C), the re-etch method (D) and the repolish method (E) (Gleadow, 1981); each method requires specific corrections for experimental factors (Section 2); (3) determining the plateau age of the Durango apatite, and (4) establishing the need, extent and appropriate method of age correction for partial annealing of the fossil tracks. The sequence of experimental steps makes it more practical to discuss population method (B) before (A).

Uranium concentration. The uranium concentration of the apatite sections was calculated from the induced-track densities in the external detectors covering the mounts during the first and second irradiations, and the corresponding thermal-neutron fluences. The equation (Table 1; Eq. 6) is that of Jonckheere (1995), Enkelmann et al. (2005a) and Hoffmann et al. (2008). Enkelmann et al. (2005a) reported partial results. Table 3 reports full details of the track counts. The concentrations were calculated with the more recent value of $g(T_n)$ (0.9832; Holden, 1999) instead of the value used before (0.977; Wagemans et al., 1988; Section 2).

Population method (*B*). In this case, the induced tracks were etched in an external apatite surface. This is the result of polishing the induced-track mounts before their irradiation. This method differs from the familiar population method (A; Gleadow, 1981) in that each population consists of an apatite section, within which random fields were counted. It nevertheless has the essential feature of a population method, i.e. counting of the fossil and induced tracks in separate apatite aliquots (sections), one of which was annealed before neutron irradiation. In contrast to the familiar population method (A), it requires a correction factor ($Q = [\eta q]_I/[\eta q]_S$) for the different etching and counting efficiencies of the fossil and induced tracks. The relevant ηq-values are from Jonckheere and Van den haute (2002) and Jonckheere (2003b) and summarized in Table 1. The age calculation also requires a correction factor (U) for the difference between the uranium concentrations of the apatite sections with fossil and induced tracks. U was calculated from the uranium concentrations in Table 3. The age calculation is summarized in Tables 4 and 5.

Population method (*A*). The fossil-track counts for this dating method are the same as for the above method (B). The sections with the induced tracks were repolished and re-etched under the same conditions as before. This obviates the need for the factor Q as the fossil and induced tracks are now both counted in an internal apatite surface. Population method (A) is equivalent to the familiar method from a methodological perspective. In spite removing 50 μm from the surface of the sections with induced tracks, it is assumed that the same uranium correction applies as for method (B). The results are listed in Tables 4 and 5.

External-detector method (*C*). The fossil-track counts are the same as before. The induced tracks were counted in external detectors covering the sections with fossil tracks during the second irradiation. This method differs from the familiar external-detector method in that no effort is made to count the fossil and induced tracks in matching areas. From the perspective of the methodological factors (Section 2), it is nevertheless equivalent. The age calculation involves G, $Q = [\eta q]_I/[\eta q]_S$, and R. In this case, $[\eta q]_I$ refers to the track counts in the mica external detectors, in contrast to the population method (B) and the re-etch method (D), where it refers to track counts in the external apatite surface. The relevant correction factors (Jonckheere, 2003b) and external-detector ages are summarized in Tables 4 and 5.

Re-etch method (*D*). The fossil-track counts are the same as before. The basal and prism section with fossil tracks were re-etched for 60 s in 2.5% HNO_3 at 25 °C, revealing the induced tracks of the second irradiation and increasing the total etch time of the fossil tracks to 120 s. The induced-track densities are given by: $\rho_I = \rho_{I+S} - T\,\rho_S$ (T: etch-time factor). Because the induced tracks were etched in an external surface, G and Q are needed (Tables 4 and 5).

Repolish method (*E*). The fossil-track counts are the same as before. The basal and prism sections were repolished and re-etched (60 s in 2.5% HNO_3 at 25 °C), revealing the combined fossil and induced tracks in internal surfaces. The induced-track densities were calculated by subtraction: $\rho_I = \rho_{I+S} - \rho_S$. The age calculations do not require G, T, Q or R (Tables 4 and 5).

Plateau age. The age of the unannealed reference sample is that obtained before with the population method (A). The data for the age plateau were obtained on the pairs of basal and prism sections with fossil and induced tracks annealed together between the two irradiations (Fig. 1). The age calculation is as for population method (A), including a correction (U) for the uranium concentrations of sections with fossil and induced tracks (Table 6).

4. Results and discussion

4.1. Uranium concentration

The uranium concentrations calculated with Eq. (6) in Table 1 are listed in Table 3. The differences with an earlier equation

Table 3
Calculation of the uranium concentrations of the Durango apatite samples; N: number of counted tracks; n: number of counted fields (1 field = 6.87 10^5 cm^2); ρ_{ED} (10^5 cm^{-2}): induced-track densities in the mica external detectors; σ/σ_P: ratio of the standard deviation of the track density distribution to that of a Poisson distribution; ϕ (10^{15} cm^{-2}): thermal-neutron fluence; ρ_{ED}/ϕ (tracks/10^{10} neutrons); $[U]_{FT}$ (ppm): uranium concentration calculated from ρ_{ED}/ϕ using Eq. (6); $[U]_{NA}$ (ppm): uranium concentrations determined by epithermal-neutron-activation analysis. Errors are 1σ.

Mica ED	Section	N	n	ρ_{ED}	σ/σ_P	ϕ_S	ρ_{ED}/ϕ_S	$[U]_{FT}$	$[U]_{NA}$
MSB 025	Basal	2929	255	1.67 ± 0.03	1.01	1.22 ± 0.02	1.37 ± 0.04	9.22 ± 0.45	9.17 ± 0.07
MIB 025	Basal	2990	229	1.90 ± 0.03	0.97	1.32 ± 0.03	1.44 ± 0.04	9.68 ± 0.47	9.35 ± 0.15
MSB 250	Basal	3309	258	1.87 ± 0.04	1.12	1.21 ± 0.02	1.54 ± 0.05	10.38 ± 0.50	
MIB 250	Basal	3128	234	1.95 ± 0.04	1.07	1.31 ± 0.03	1.48 ± 0.04	9.99 ± 0.48	
MSB 300	Basal	3464	212	2.38 ± 0.04	0.96	1.20 ± 0.02	1.98 ± 0.05	13.33 ± 0.64	
MIB 300	Basal	4175	230	2.64 ± 0.04	1.03	1.30 ± 0.03	2.03 ± 0.05	13.67 ± 0.65	
MSB 350	Basal	3543	216	2.39 ± 0.04	1.06	1.18 ± 0.02	2.02 ± 0.05	13.61 ± 0.65	
MIB 350	Basal	4062	232	2.55 ± 0.04	1.09	1.30 ± 0.03	1.96 ± 0.05	13.19 ± 0.63	
MSP 025	Prism	3860	254	2.21 ± 0.04	1.11	1.22 ± 0.02	1.81 ± 0.05	12.20 ± 0.59	12.18 ± 0.18
MIP 025	Prism	3860	237	2.37 ± 0.04	1.01	1.31 ± 0.03	1.81 ± 0.05	12.17 ± 0.58	12.05 ± 0.31
MSP 250	Prism	3297	211	2.27 ± 0.04	1.09	1.20 ± 0.02	1.89 ± 0.05	12.75 ± 0.62	
MIP 250	Prism	3512	212	2.41 ± 0.04	0.96	1.31 ± 0.03	1.84 ± 0.05	12.38 ± 0.59	
MSP 300	Prism	2536	207	1.78 ± 0.04	1.09	1.19 ± 0.02	1.50 ± 0.04	10.08 ± 0.50	
MIP 300	Prism	2900	223	1.89 ± 0.04	1.05	1.30 ± 0.03	1.46 ± 0.04	9.79 ± 0.48	
MSP 350	Prism	2526	222	1.66 ± 0.04	1.09	1.18 ± 0.02	1.40 ± 0.04	9.44 ± 0.47	
MIP 350	Prism	3091	227	1.98 ± 0.04	0.96	1.29 ± 0.03	1.54 ± 0.04	10.33 ± 0.50	

(Enkelmann et al., 2005a; Hoffmann et al., 2008; Jonckheere, 1995) are the new Westcott g-factor (0.9832; Holden, 1999) and the correction ($\beta = 1.0025$; Jonckheere, 1995) for the difference between the Westcott and Høgdahl formalisms. Their combined effect is <1%. Table 3 also reports the uranium concentrations of four sections determined with epithermal-neutron-activation analysis (ENAA; Bellemans, Institute for Nuclear Sciences, Universiteit Gent). These are on average 1.3% lower, half of which is attributable to one sample. The good agreement supports the value of the ηq-factor in Eq. (6) ($[\eta q]_{ED} = 0.91 \pm 0.01$; Table 1), which implies that the efficiency of induced-track counts in muscovite external detectors is far lower than 100%. This indicates that ηq is not a function of the bulk-etch rate but of the fraction of shallow tracks ($z < 0.5$ μm; Jonckheere and Van den haute, 2002) approaching the optical contrast limit of the microscope. These results further endorse that the induced-track density in an external detector is not proportional to the etchable track length in the irradiated mineral but to that in the detector, corrected for the length deficit in both (Jonckheere, 2003b). The uranium results can also be interpreted as evidence for accurate neutron-fluence determinations with the aid of dilute metal-activation monitors (Au, Co). It is important that this evidence is not affected by the interdependence of ϕ and λ_F (ϕ/λ_F-problem), which has long been considered an unsurmountable obstacle to standardless dating, and heralded the ζ-calibration (Hurford, 1990a, b, 1998; Hurford and Green, 1981, 1983).

The uranium concentrations in Table 3 give an indication of the uranium distribution at different scales. The ratios of the standard deviations of the track-density distributions to those of the corresponding Poisson distributions (σ/σ_P) are on average somewhat higher than 1 (mean: 1.04), indicating the absence of substantial uranium inhomogeneities at the scale of the counting grid (>0.01 mm^2). The ratio of the standard deviations of the values for the four sections from each crystal to their average statistical uncertainties is of the same order (mean: 1.11), allowing a similar conclusion concerning uranium inhomogeneities between sections at the scale of the areas counted within each (>1 mm^2). In contrast, the differences between crystals (up to 30%) are much larger than the variation within each (standard-deviation ratio >10), as noted by Naeser and Fleischer (1975).

4.2. Apparent fission-track age

Table 1 lists the equations and the physical and empirical constants used for calculating the fission-track ages without (Eq. 7; population and external-detector methods) and with subtraction (Eq. 8; re-etch and repolish methods). No annealing correction is involved at this stage; the results are thus apparent ages, not corrected for shortening of the fossil tracks ($L = 1$). Table 4 summarizes the track counts and neutron fluences and lists the results of a conventional age calculation, i.e. leaving out the method-specific corrections for experimental factors

Table 4
Conventional calculation of the fission-track age of the Durango apatite. A: population method with induced-track counts in an internal apatite section; B: population method with induced-track counts in an external apatite surface; C: external-detector method; D: re-etch method; E: repolish method; $[RG]_S$, $[RG]_I$: registration geometries of the fossil tracks (S) and induced (I) tracks (IS: internal section; ES: external surface; ED: external detector); N_S, N_I: fossil (S) and induced (I) tracks counts; n_S, n_I: number of fields counted for the fossil (S) and induced (I) tracks (IS and ES: 1 field = 6.16 10^{-5} cm^2; ED: 1 field = 6.87 10^{-5} cm^2); ρ_S, ρ_I (10^5 cm^{-2}): surface-track densities of the fossil (S) and induced (I) tracks (*: $\rho_S + \rho_I$); ϕ_S (10^{15} cm^{-2}): Høgdahl thermal-neutron fluence; $[t_{FT}]_C$ (Ma): conventional fission-track age. Errors are 1σ.

Method	Section	$[RG]_S$	N_s	n_S	ρ_S	$[RG]_I$	N_I	n_I	ρ_I	ϕ_S	$[t_{FT}]_C$
A	Basal	IS	2205	246	1.45 ± 0.03	IS	4265	219	3.16 ± 0.05	1.32 ± 0.03	29.6 ± 1.0
A	Prism	IS	3172	267	1.93 ± 0.04	IS	4610	190	3.94 ± 0.06	1.31 ± 0.03	31.3 ± 1.0
B	Basal	IS	2205	246	1.45 ± 0.03	ES	2500	225	1.80 ± 0.04	1.32 ± 0.03	26.0 ± 1.0
B	Prism	IS	3172	267	1.93 ± 0.04	ES	2907	219	2.15 ± 0.04	1.31 ± 0.03	28.6 ± 1.0
C	Basal	IS	2205	246	1.45 ± 0.03	ED	2929	255	1.67 ± 0.03	1.22 ± 0.02	25.9 ± 0.9
C	Prism	IS	3172	267	1.93 ± 0.04	ED	3860	254	2.21 ± 0.04	1.22 ± 0.02	25.9 ± 0.9
D	Basal	IS	2205	246	1.45 ± 0.03	ES	2226	123	*2.94 ± 0.07	1.22 ± 0.02	29.2 ± 1.1
D	Prism	IS	3172	267	1.93 ± 0.04	ES	3264	116	*4.57 ± 0.08	1.22 ± 0.02	21.8 ± 0.7
E	Basal	IS	2205	246	1.45 ± 0.03	IS	5293	204	*4.21 ± 0.06	1.22 ± 0.02	31.4 ± 1.1
E	Prism	IS	3172	267	1.93 ± 0.04	IS	3837	105	*5.93 ± 0.10	1.22 ± 0.02	28.7 ± 1.0

discussed in Section 2. In practice this means that $G = ½$ or 1, depending on the method, $Q = 1$, $R = 1$, and $T = 1$. Although U is a sample-specific factor and not a fundamental methodological one, it was also assumed that $U = 1$ for simplicity. The conventional ages exhibit a much greater spread (21.8 ± 0.7 to 31.4 ± 1.1 Ma; Table 4; Fig. 2) than their errors permit. Their mean (27.8 ± 0.9 Ma) is >10% lower than the reference age (31.4 ± 0.5 Ma; Green, 1985; Hurford, 1990a, b). It is striking that the common population (A; mean 30.5 ± 0.8 Ma) and repolish methods (E; mean 30.0 ± 1.4 Ma), neither of which requires methodological corrections, give ages within <2σ of the reference age.

Table 5 lists the apparent fission-track ages based on the same track counts (Table 4), but calculated with the correction factors discussed in Section 2, together with their values calculated from the data in Tables 1 and 3. G depends on the method used (½ or 1). R is constant for apatite dated using muscovite external detectors, but takes a different value for other minerals or other external detectors. Q and T, in contrast, are specific to the etching and observation conditions and the track identification criteria of the microscope operator. Q and T are also expected to be different for other apatite sections than basal and prism faces. U is specific to the samples and experimental procedure in this work. In contrast to the conventional ages, the corrected apparent ages determined with the different dating methods are consistent with each other and the reference age (Table 5). The results range from 28.7 ± 1.0 Ma to 32.0 ± 1.7 Ma with a mean of 30.9 ± 0.3 Ma, <2% lower than the reference age. Their standard deviation (0.9 Ma) is less than the calculated uncertainties of the individual ages. This is expected because the fossil-track counts are the same for all dating methods and some correction factors are common to two or more age calculations. The same applies to the neutron fluences because a single fluence, albeit corrected for minor fluence gradients, was determined for each of the two sample irradiations.

Earlier studies (Bellemans, 1996; Bigazzi et al., 1990; Curvo et al., 2013; De Corte et al., 1991, 1995; Jonckheere, 1995; Van den haute et al., 1988, 1998) give reason for trusting that the calculated neutron fluences are accurate. The agreement of the uranium concentrations calculated with Eq. (6) with independent data (Enkelmann et al., 2005a; Hoffmann et al., 2008; Section 4.1) supports this assumption. It is reasonable to conclude from re-evaluations of the ^{238}U-fission constant (Holden, 1989; Holden and Hoffman, 2000) that the value used is also accurate. The fact that the correction factors introduced in Section 2 remove the inconsistencies between the ages obtained with different dating methods is a convincing argument for concluding that these are needed and accurate within their uncertainties. It is reasonable to conclude that the agreement of the mean apparent age (30.9 ± 0.6 Ma; 2σ) with the reference age (31.4 ± 0.5 Ma; 2σ) is not fortuitous. However, this runs counter to the current consensus, implemented in all modelling algorithms, which requires that a shortening of the fossil-track length of 10% or more, relative to the length of the induced tracks, implies a proportional lowering of the apparent fission-track age (Crowley, 1993; Green, 1988; Guedes et al., 2004; Jones and Dokka, 1990; Ketcham, 2005; Laslett et al., 1984; Lutz and Omar, 1991; Tello et al., 2006; Watt and Durrani, 1985; Willett, 1997).

4.3. Length-corrected age

The mean lengths of fossil and induced confined tracks etched in prism faces of the Durango apatite are l_S = 14.5 ± 0.1 μm and l_I = 16.3 ±0.1 μm (Jonckheere and Van den haute, 2002), in good agreement with most published data, including for different etching conditions (Table 2). In this case, $L = l_I/l_S$ (= 1.12 ± 0.01) is a close lower estimate of the correction factor entered in Eqs. (7) and (8) (Table 1) for calculating the length-corrected ages. For approximate isothermal holding, this estimate is almost independent of the annealing model and the length-bias model (ρ/ρ_0 vs. l/l_0) (Wauschkuhn et al., 2015a). The length-corrected ages, including the corrections for methodological factors, are listed in Table 5. The ages obtained with different dating methods are still consistent with each other, but none is in agreement with the reference age of the Durango apatite. The mean length-corrected age (34.7 ± 0.3 Ma) overestimates the reference age by almost 10 standard errors, whereas the mean uncorrected age underestimates it by less than two.

It appears that the apparent fission-track age of the Durango apatite requires no, or at most a small, correction. This is also the case for the Fish Canyon tuff standard (Enkelmann et al., 2005b). Green (1988) made the same observation for apatites with "volcanic type" length distributions, rapidly cooled apatites, most but not all of volcanic origin, which were not reheated. The means (14.0–15.7 μm) and standard deviations (0.8–1.3 μm) of their fossil-track-length distributions indicate moderate ambient-temperature annealing (Gleadow et al., 1986). Green (1988) ascribed the fact that their apparent fission-track ages permitted no length correction to possible dating errors related to the efficiencies of the fossil and induced-track counts rather than to the effects of the neutron fluence or fission constant. This is not an adequate explanation of our results, considering the explicit corrections for these effects and their, at least partial, success at bringing the results of different dating methods and those for basal and prism sections in line with each other and with the reference age.

Gleadow and Duddy (1981) and Gleadow et al. (1983) proposed an explanation based on their investigation of borehole samples from the Australian Otway Basin. Their "ageing" concept holds that fossil tracks in apatite undergo length reductions up to 15–20% under geological annealing at <70 °C without attendant lowering of its apparent fission-track age. Although the concept was abandoned, ageing could account for our dating results. Ageing lost favour because Green

Table 5
Calculation of the fission-track age of the Durango apatite, corrected for experimental factors. A: population method with induced-track counts in an internal section; B: population method with induced-track counts in an external surface; C: external-detector method; D: re-etch method; E: repolish method; $[t_{FT}]_C$ (Ma): conventional fission-track age (Table 3); $[t_{FT}]_{CL}$ (Ma): length-corrected conventional age; $Q = [\eta q]_I/[\eta q]_S$: correction factor for the different counting efficiencies of the fossil (S) and induced (I) tracks (calculated from ηq-values in Jonckheere and Van den haute, 2002; Table 1); R: correction factor for the different length deficit of induced tracks in apatite and muscovite (Jonckheere, 2003b); T: correction factor for the different etch times of the fossil and induced tracks (Jonckheere and Van den haute, 1996); U: correction factor for the different uranium contents of the apatite sections with fossil and induced tracks (Table 3); L: correction factor for the different etchable lengths of fossil and induced tracks (confined-track lengths in Jonckheere and Van den haute, 2002); $[t_{FT}]_A$ (Ma): apparent fission-track age; $[t_{FT}]_{AL}$ (Ma): length-corrected age. Errors are 1σ.

Meth.	Sect.	$[t_{FT}]_C$	$[t_{FT}]_{CL}$	G	Q	R	T	U	L	$[t_{FT}]_A$	$[t_{FT}]_{AL}$
A	Basal	29.6 ± 1.0	33.3 ± 1.2	1	1	1	1	1.05 ± 0.04	1.12 ± 0.01	31.1 ± 1.6	35.0 ± 1.8
A	Prism	31.3 ± 1.0	35.2 ± 1.2	1	1	1	1	0.99 ± 0.04	1.12 ± 0.01	31.2 ± 1.5	35.1 ± 1.7
B	Basal	26.0 ± 1.0	29.2 ± 1.1	½	1.12 ± 0.02	1	1	1.05 ± 0.04	1.12 ± 0.01	30.6 ± 1.7	34.4 ± 1.9
B	Prism	28.6 ± 1.0	32.1 ± 1.1	½	1.12 ± 0.02	1	1	0.99 ± 0.04	1.12 ± 0.01	32.0 ± 1.7	35.9 ± 1.9
C	Basal	25.9 ± 0.9	29.1 ± 1.1	½	1.00 ± 0.02	1.21 ± 0.02	–	1	1.12 ± 0.01	31.3 ± 1.5	35.2 ± 1.7
C	Prism	25.9 ± 0.9	29.2 ± 1.0	½	1.00 ± 0.02	1.21 ± 0.02	–	1	1.12 ± 0.01	31.4 ± 1.4	35.3 ± 1.6
D	Basal	29.2 ± 1.1	32.8 ± 1.2	½	1.12 ± 0.02	1	0.94 ± 0.03	1	1.12 ± 0.01	30.9 ± 1.6	34.7 ± 1.8
D	Prism	21.8 ± 0.7	24.4 ± 0.8	½	1.12 ± 0.02	1	1.26 ± 0.04	1	1.12 ± 0.01	30.1 ± 1.5	33.8 ± 1.7
E	Basal	31.4 ± 1.1	35.3 ± 1.2	1	1	1	1	1	1.12 ± 0.01	31.4 ± 1.1	35.2 ± 1.2
E	Prism	28.7 ± 1.0	32.2 ± 1.1	1	1	1	1	1	1.12 ± 0.01	28.7 ± 1.0	32.2 ± 1.1
Mean:		27.8 ± 0.9	31.3 ± 1.1							30.9 ± 0.3	34.7 ± 0.3

(1988) argued that it was an artefact. The ages of the borehole samples (t) had indeed been normalized to that of a surface sample (t_0), that exhibited a length reduction ($l_{S0} < l_I$) relative to induced tracks (l_I). After renormalizing ($[t/t_0] \rightarrow [l_{S0}/l_I] \times [t/t_0]$), the Otway data were found to be in agreement with the (ρ/ρ_0 vs. l/l_0)-trend of induced tracks. An objection to Green's (1988) renormalization is that it assumed what it proved. Renormalization is acceptable if ageing is indeed an artefact. However, if it is not, then the renormalization itself is invalid, and the data remain unchanged, corroborating that ageing is real. A second objection is that the observation that the renormalized (ρ/ρ_0 vs. l/l_0)-trend for fossil tracks coincides with that for induced tracks does not permit to conclude that the same annealing mechanism operates in both cases. The two trends cannot be assumed to coincide for the same reason that the trend for multicompositional apatites lies above that for monocompositional apatites (Green, 1988). A third argument against renormalization is that the renormalized apatite ages of outcrop samples are ca. 10% older than the titanite fission-track ages of the same volcanoclastic rocks. Barring unknown systematic errors of the right magnitude affecting one but not the other (excluding ϕ and λ_F), this is as strong an argument for ageing as the former, establishing that Green's (1988) case is inconclusive, but not that it is invalid.

4.4. Plateau-age experiment

Our length measurements confirm the shortening of the fossil tracks in the Durango apatite (Table 2) but theory is inconclusive as to whether or not an age correction is required. An attempt was therefore made to determine the corrected age of the Durango apatite with the plateau method of Storzer and Poupeau (1973). This method is almost never used but can be shown to be valid within the current paradigm of the fission-track method. Numerical calculations based on the Markov assumption (equivalent time; Duddy et al., 1988) and an annealing model (e.g. Laslett et al., 1987) indicate that, if the age correction implied by the confined-track lengths is needed, then an age plateau exists at 35.3 Ma at temperatures upward of ca. 250 °C (for 1 h annealing; Jonckheere, 2003a). Moreover, the plateau method does not depend on a specific, or known, (ρ/ρ_0 vs. l/l_0)-relationship or on the assumption that the same relationship holds for geological annealing of fossil fission tracks and lab annealing of induced tracks. Instead, it rests on the lesser condition that, when the fossil and induced tracks have been annealed together to the same length in the lab, the corresponding surface-track densities have also been reduced to the same fraction.

The plateau ages were calculated with Eq. (7) (Table 1), with $G = 1$, $Q = 1$, $R = 1$, and U based on the uranium concentrations in Table 3, and are listed in Table 6 and plotted in Fig. 3. There is a clear distinction between the ages of the samples annealed at 350 °C and at those annealed

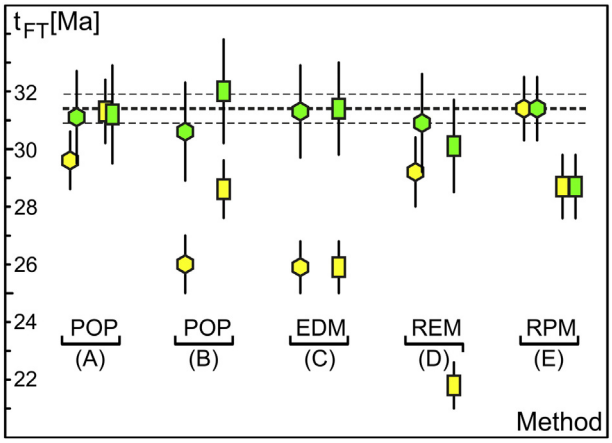

Fig. 2. Dating results obtained on basal and prism sections of the Durango apatite with the population (A, B; see text), external detector (C), re-etch (D) and repolish methods (E). Hexagons: basal sections; rectangles: prism sections; yellow: conventional age calculation ($[t_{FT}]_C$: Table 4); green: ages corrected for experimental factors but not for partial annealing of the fossil tracks ($[t_{FT}]_A$: Table 5); error bars are 1σ. Dashed lines: reference age and 2σ confidence interval. A conventional age calculation gives inconsistent results, of which only a fraction is in agreement with the reference age. Corrections for method-related experimental factors bring the fission-track ages in line with each other and with the reference age.

250 and 300 °C. This is also so for the data of Naeser and Fleischer (1975) and for the annealing data of Green (1988) for the Renfrew and Otway apatites, although not at exactly 350 °C. Annealing for 1 h at 350 °C brings the tracks to the point at which unetchable gaps appear (Green et al., 1986) or where tracks at high angles to the c-axis undergo accelerated length reduction (Donelick, 1991; Donelick et al., 1999). The distinction is not crucial because the relationship between the volumetric and surface-track densities breaks down in either case. Projected-length measurements of the fossil and induced tracks in the samples annealed at 350 °C revealed an excess of short tracks that is reduced but not eliminated by an additional etch (25 s; 2.5% HNO_3; 25 °C; Jonckheere, 1995). This has unpredictable effects on the surface-track densities and results in erratic ages.

The mean age of the samples annealed at 250 and 300 °C (plateau age; 31.4 ± 0.7 Ma) is indistinguishable from that of the unannealed samples (Table 6; 31.2 ± 0.7 Ma), the mean of all dating methods (Table 5; 30.9 ± 0.3 Ma) and from the reference age (31.4 ± 0.5 Ma; 2σ). This suggests that no, or at most a small (<2%), age correction is required and excludes the much larger correction (>12%) required by the measured mean confined-track lengths.

Table 6
Calculation of the fission-track age plateau of the Durango apatite. T (°C): 1 h annealing temperature (*: samples etched additional 25 s); N_S, N_I: fossil (S) and induced (I) tracks counts; n_S, n_I: number of fields counted for the fossil (S) and induced (I) tracks (1 field = 6.16 10^{-5} cm^2); ρ_S, ρ_I (10^5 cm^{-2}): surface-track densities of the fossil (S) and induced (I) tracks; U: correction factor for the different uranium concentrations of the apatite sections with fossil and induced tracks;ϕ_S (10^{15} cm^{-2}): Høgdahl thermal-neutron fluence; $[t_{FT}]_A$ (Ma): apparent fission-track age. Errors are 1σ.

T	Section	N_S	n_S	ρ_S	N_I	n_I	ρ_I	U	ϕ_S	$[t_{FT}]_A$
~25	Basal	2205	246	1.45 ± 0.03	4265	219	3.16 ± 0.05	1.05 ± 0.04	1.32 ± 0.03	31.1 ± 1.7
~25	Prism	3172	267	1.93 ± 0.04	4610	190	3.94 ± 0.06	0.99 ± 0.04	1.31 ± 0.03	31.2 ± 1.6
250	Basal	1499	159	1.52 ± 0.04	2020	106	3.09 ± 0.07	0.96 ± 0.04	1.31 ± 0.03	30.4 ± 1.8
250	Prism	3118	262	1.93 ± 0.03	4894	211	3.76 ± 0.06	0.98 ± 0.04	1.31 ± 0.03	31.8 ± 1.6
300	Basal	2225	214	1.69 ± 0.04	2307	107	3.50 ± 0.07	1.02 ± 0.04	1.30 ± 0.03	31.3 ± 1.7
300	Prism	2626	330	1.29 ± 0.03	3479	228	2.48 ± 0.04	0.97 ± 0.05	1.30 ± 0.03	32.1 ± 1.8
									Mean:	31.4 ± 0.7
350	Basal	1615	255	1.03 ± 0.03	2281	150	2.47 ± 0.06	0.98 ± 0.03	1.30 ± 0.03	25.6 ± 1.4
350	Prism	2318	404	0.93 ± 0.02	2884	270	1.73 ± 0.03	1.08 ± 0.04	1.29 ± 0.03	37.0 ± 2.0
350*	Basal	1896	306	1.01 ± 0.02	3210	209	2.49 ± 0.05	0.98 ± 0.03	1.30 ± 0.03	24.8 ± 1.3
350*	Prism	1843	270	1.11 ± 0.03	2216	202	1.78 ± 0.04	1.08 ± 0.04	1.29 ± 0.03	42.8 ± 2.4

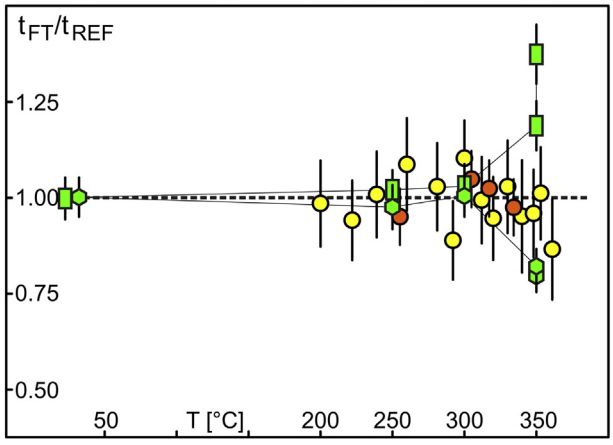

Fig. 3. Plateau-age results for the Durango apatite normalized to the reference age. Green hexagons: basal sections, green rectangles: prism sections (this work). Orange circles: data of Naeser and Fleischer (1975) for <350 °C; yellow circles: plateau ages calculated from the annealing data of Green (1988). The error bars are 1σ. Excluding the erratic ages at 350 °C, which are due to accelerated length reduction or break-up of the tracks, the plateau ages of the Durango apatite are consistent with its reference age, indicating that no length correction is required.

4.5. Effective track lengths

It appears that there is a contradiction between the mean confined-track lengths (l) and the dating results based on surface-track densities (ρ). These are not independent of each other but related through the equation of Price and Walker (1963): $\rho = ½\, l\, N$, applicable to both fossil and induced tracks etched in an internal apatite section. The volumetric track densities (N) can be calculated for the four samples for which we have independent estimates of the uranium concentration (Table 3). Converting the ppm-concentrations to atoms per volume and factoring in the isotopic abundances (θ_{235}; $\theta_{238} = 1 - \theta_{235}$; Table 1) gives the isotope concentrations, U_{238} and U_{235}, in Eqs. (2) and (3). These equations then give the volumetric densities of fossil (N_S) and induced (N_I) tracks, if the sample age and neutron fluence are known. From N_S and N_I and the surface-track densities ρ_S and ρ_I, we can then calculate the effective etchable lengths of the fossil (l_{S0}) and induced (l_{I0}) tracks: $l_{S0} = 2\rho_S/N_S$ and $l_{I0} = 2\rho_I/N_I$. The full equations, with corrections for the Høgdahl neutron fluence (ϕ_S) and the track registration (g_{IS}), etching and counting efficiencies ($[\eta q]_{IS}$), are given in Table 1 (Eqs. 9 and 10). The calculation assumes that l_{S0} and l_{I0} are isotropic. The equations of Ketcham et al. (2007) confirm that this is a good approximation for fossil ($l_A/l_C = 0.94$; l_A and l_C: mean track lengths perpendicular and parallel to the apatite c-axis) and induced tracks ($l_A/l_C = 0.99$) in the Durango apatite.

Table 7 lists the calculated effective lengths. Their ratio $L = l_{I0}/l_{S0}$ is not independent of the dating results as it is that which gives the exact reference age when substituted in the age equation (Section 2). The values of l_{S0} and l_{I0} are not fixed by the dating results. The mean effective length of the induced tracks ($l_{I0} = 16.8 \pm 0.4$ μm) agrees within error with most confined-track-length measurements using our and other etching conditions (Table 2). It agrees somewhat better with values obtained after longer etch times or for tracks etched minutes after irradiation (Donelick et al., 1990). The mean effective length of the fossil tracks ($l_{S0} = 16.3 \pm 0.4$ μm) is ca. 0.5 μm less than that of the induced tracks but consistent with it within error. It is however not consistent with values based on confined-track-length measurements, which are on average ca. 2 μm lower (Table 2). This confirms that the shortening of the fossil confined tracks in the Durango apatite and, by extension, in age standards and apatites with volcanic-type length distributions has no, or at most a small, effect on their fossil-track densities, and hence on their fission-track ages. This supports the interpretation of Gleadow and Duddy (1981) and Gleadow et al. (1983) and contradicts the current consensus implemented in the fission-track modelling programs.

4.6. Independent evidence

The standardless fission-track ages of the Durango apatite, determined with different dating procedures, with proper corrections for the associated experimental factors, but without correction for the shortening of the fossil confined tracks, are in near-agreement with its reference age. It is nevertheless difficult to dispel the suspicion that there exist unknown methodological factors causing these ages to be overestimated by the exact amount required by the fossil and induced confined-track lengths (Green, 1988). Independent confirmation is provided by considerations unrelated to the complexities of fission-track dating. It is known that the apatite (U,Th)/He system is, in general, less retentive than the fission-track system. Although the order is reversed below ca. 35 °C, depending on the diffusion and annealing model, the difference is small. Moreover, the track-annealing models refer to the shortening of the confined-track length, which, according to our findings, must not involve an equal lowering of the fission-track age. Therefore, the fact that a sample's (U,Th)/He age has not been lowered relative to that determined with high-temperature thermochronometers is a strong indication that its fission-track age has not been lowered either. Although this is the case for the Durango apatite (Table 2), its exceptional crystal size implies that significant (≥5%) He loss requires temperatures in excess of ca. 75 °C (Durango diffusion kinetics; equivalent spherical radius 5 mm; 30 Ma isothermal holding). The argument is therefore inconclusive in the specific case of the Durango apatite.

The case is instead proved by the apatite (U,Th)/He ages of the Fish Canyon Tuff, which are concordant with U/Pb and Ar/Ar ages dating its eruption at ca. 28 Ma (Gleadow et al., 2015, and references therein). At the classic sampling site of this age standard, the (U,Th)/He age (20.8 ± 0.4 Ma) is lowered due to protracted cooling in the temperature range 40–60 °C but the LA-ICP-MS fission-track age (28.8 ± 0.8 Ma) is

Table 7
Calculation of the effective lengths of induced (l_{I0}; μm) and fossil (l_{S0}; μm) tracks in the Durango apatite; $N_{I,S}$: number of induced and fossil tracks; $n_{I,S}$: number of fields counted for the induced and fossil-track counts; $\rho_{I,S}$ (10^5 cm^{-2}): areal densities of induced and fossil tracks; $[U]_{ENAA}$ (ppm): uranium concentration determined with epithermal-neutron-activation analysis; ϕ_S (10^{15} cm^{-2}): Høgdahl subcadmium neutron fluence calculated from the activities of co-irradiated metal-activation monitors; $[t]_{REF}$ (Ma): reference age of the Durango apatite. Errors are 1σ.

Induced tracks							
Sample	Section	N_I	n_I	ρ_I	$[U]_{ENAA}$	ϕ_S	l_{I0}
DIB 025	Basal	4265	219	3.16 ± 0.05	9.35 ± 0.15	1.32 ± 0.03	17.0 ± 0.6
DIP 025	Prism	4610	190	3.94 ± 0.06	12.05 ± 0.31	1.31 ± 0.03	16.5 ± 0.7 16.8 ± 0.4
Fossil tracks							
Sample	Section	N_S	n_S	ρ_S	$[U]_{ENAA}$	$[t]_{REF}$	l_{S0}
DSB 025	Basal	2205	246	1.45 ± 0.03	9.17 ± 0.07	31.4 ± 0.3	16.3 ± 0.6
DSP 025	Prism	3172	267	1.93 ± 0.04	12.18 ± 0.16	31.4 ± 0.3	16.3 ± 0.5

not. The latter is consistent with the mean LA-ICP-MS fission-track age (28.2 ± 0.5 Ma; Gleadow et al., 2015) and standardless external-detector ages (27.7 ± 0.5 Ma; Enkelmann et al., 2005b; 27.3 ± 0.5 Ma; Iwano, pers. com.). This establishes that the apatite (U,Th)/He method is more temperature sensitive than the fission-track method, in accord with the small grain size of the Fish Canyon Tuff compared to Durango. Therefore, except at the classic sampling site, the fission-track ages cannot be lower than the emplacement age dated with the (U,Th)/He and other thermochronometers. This conflicts with the mean fossil confined-track length (14.84 ± 0.04 μm; Gleadow et al., 2015) requiring a correction of ca. 10%, giving a length-corrected age > 31 Ma, which is irreconcilable with the emplacement age. The same reasoning and conclusion apply to the Limberg t3 proposed apatite age standard (mean sanidine Ar/Ar age: 16.3 ± 0.2 Ma; mean titanite (U,Th)/He age: 16.5 ± 0.5 Ma; mean apatite (U,Th)/He age: 16.8 ± 1.0 Ma (grain size 300–500 μm); mean fossil-track length: 15.2 ± 0.1 (1σ) μm, theoretically requiring a age correction of ca. 7%; Kraml et al., 2006).

5. Summary and conclusions

Five dating strategies were used for determining the standardless fission-track age (ϕ-age) of the Durango apatite, differing in the manner in which the induced-track densities are measured. A conventional calculation, ignoring experimental factors, gives inconsistent ages with method-related differences >15%. Correcting for these method-specific experimental factors brings them in line with each other and with the reference age, but leaves no margin for a correction based on the mean fossil confined-track length. Three observations suggest that such a correction is indeed inappropriate. (1) The evidence for age corrections based on the mean confined-track lengths is shown to be inconclusive. (2) The plateau age of the Durango apatite is consistent with its apparent age to within 1%. (3) The calculated effective etchable length of the fossil fission tracks agrees within error with that of the induced tracks; both are also in agreement with the measured length of induced confined tracks. Moreover, although the specific case of the Durango apatite is inconclusive, the fact that the (U,Th)/He ages of dated age standards are consistent with their reference ages, leaves no margin for a lowered fission-track age resulting from partial annealing.

The corrections for experimental factors specific to the dating method and analyst imply that – like the ζ-calibration – standardless fission-track dating, in general, requires a personal empirical calibration factor. However, for the population method (A) and repolish method (E), it is reasonable to assume that the overall experimental factor is equal 1 for samples homogenous in uranium. For all dating methods, the calibration factor can be determined using age standards, in which case the method ceases to be standardless but becomes a deconvoluted ζ-method (Hurford, 1998). On the other hand, it is also possible to construct the calibration factor from its components (G, Q, R, T; Jonckheere, 2003b; Enkelmann and Jonckheere, 2003; Enkelmann et al., 2005b; Soares et al., 2013) or to combine both these approaches in a single multiple calibration (ζ_0-method: Jonckheere, 2003b). The ζ-method has the advantage of eliminating the need for neutron-fluence measurements but the disadvantage that the substituting track counts (ρ_D) in micas irradiated against standard uranium glasses lack the resolution for detecting all but large neutron-fluence gradients. The ε-method (Hasebe et al. 2004) and ξ-method (Gleadow et al., 2015), standardless dating methods in which the neutron irradiation and induced-track counts are replaced by mass-spectrometric uranium measurements, require the same attention to the track-counting efficiencies as the standardless ages determined in this work, and the question of the effective length of the fossil tracks cannot be ignored. These experimental factors can be sidestepped by calibration against age standards (ζ_{MS}-method; Hasebe et al., 2013). The ζ-method still appears to be the only accepted option for dating titanite, zircon and minerals more sensitive to irradiation damage than apatite. However, Danhara and Iwano (2013) and Iwano (pers. com., in part based on Iwano and Danhara, 1998) reported standardless fission-track dating of zircon and titanite with the external-detector method, despite the added complications caused by radiation damage effects.

The recommendation of the ζ-calibration by the Fission Track Working Group of the I.U.G.S. Subcommission on Geochronology (Hurford, 1990a, b) has thus served as much to circumvent experimental factors related to track registration, revelation and counting as to circumvent the ϕ/λ_F-problem (Hurford and Green, 1981, 1983). This meant that these problems remained unresolved but supported countless geological applications. The fact that the fission-track ages of the age standards need no correction for partial annealing explains that the ϕ- and ζ-ages of geological samples are consistent within error (De Grave and Van den haute, 2002; Enkelmann et al., 2005b, 2006; Grimmer et al., 2002; Wauschkuhn et al., 2015a). It also lends meaning to ζ-ages, which must otherwise be interpreted as part-corrected ages (Green, 1985, 1988), with an uncertain relationship to the apatite closure temperature.

The available data indicate that the conclusion that the shortened etchable length of the fossil confined tracks in the Durango apatite has no effect on its apparent fission-track age applies to other age standards (Enkelmann et al.; 2005b; Enkelmann and Jonckheere, 2003; Iwano, pers. com., in part based on data of Iwano and Danhara, 1998; Kraml et al. 2006) and apatites with a volcanic-type length distribution (Green, 1988). It is probable that it also applies to samples with a substantial component of tracks formed at low temperatures. Recent evidence shows that terminal track sections that are unetchable in the apatite grain interiors are revealed by surface-assisted sub-threshold etching at their intersection with the surface (Wauschkuhn et al., 2015b). In consequence, the etchable lengths of the confined fission tracks must not be the same as those of the surface tracks. Step-etching results (Tamer, 2012) further suggest that the apparent shortening of fossil confined tracks in the Durango apatite could be due to a lowering of the track-etch rate in geological (radiation damaged) samples. In that case, models fitted to lab-annealing data will underestimate the length reduction of the fossil confined tracks in geological samples etched under the same conditions as induced tracks. In consequence, apatite fission-track modelling programs overstretch their (T,t)-paths and overestimate palaeotemperatures in their later parts. The familiar worldwide recent exhumation is then an artefact due to a methodological imperfection rather than a consequence of selecting the annealing model of Laslett et al. (1987). It also implies that normalizing fossil-track lengths to a personal initial length (zero-length), either that of induced tracks (Ketcham et al., 2009; 2015) or that of fossil tracks considered not to have experienced significant geological annealing (Gunnell et al., 2003; Kohn et al., 2002; 2005), has unpredictable effects on the thermal histories.

Acknowledgements

Our research was carried out with support from the Belgian Institute for Research in Science and Technology (IWT) and the German Research Foundation (DFG grants JO 358/3 and RA 442/27). We are grateful to F. De Corte and A. Dewispelaere (INW, Universiteit Gent) for supervision of the neutron irradiations and assistance with the γ-spectrometric measurements. Constructive reviews by M. Danišík and H. Iwano made a significant contribution to this paper.

References

Abdullin, F., Solé, J., Solari, L., 2014. Fission-track dating and LA-ICP-MS multi-elemental analysis of the fluorapatite from Cerro de Mercado (Durango, Mexico). Rev. Mex. Cien. Geol. 31, 395–406 (in Spanish).

Afra, B., Lang, M., Rodriguez, M., Zhang, D.J., Giulian, R., Kirby, N., Ewing, R.C., Trautmann, C., Toulemonde, M., Kluth, P., 2011. Annealing kinetics of latent particle tracks in Durango apatite. Phys. Rev. 83 064116–1–5.

Alva-Valdivia, L.M., Goguitchaichvili, A., Urrutia-Fucugauchi, J., Caballero-Miranda, C., Vivallo, W., 2001. Rock-magnetism and ore microscopy of the magnetite-apatite ore deposit from Cerro de Mercado, Mexico. Earth, Planets Space 53, 181–192.

Barbarand, J., Carter, A., Wood, I., Hurford, A., 2003a. Compositional and structural control of fission-track annealing in apatite. Chem. Geol. 198, 107–137.

Barbarand, J., Hurford, A., Carter, A., 2003b. Variation in apatite fission-track length measurement: implications for thermal history modelling. Chem. Geol. 198, 77–106.

Barbarand, J., Pagel, M., 2001a. Cathodoluminescence study of apatite crystals. Am. Mineral. 86, 473–484.

Barbarand, J., Pagel, M., 2001b. Importance of the chemistry to characterise apatite fission-track annealing. C. R. Acad. Sci., Sciences de la Terre et des Planètes 332, 259–265 (in French).

Bellemans, F., 1996. A nuclear-analytical contribution to the absolute calibration of the fission-track dating method Ph.D. thesis, Universiteit Gent, 177 pp. (in Flemish).

Belousova, E.A., Griffin, W.L., O'Reilly, S.Y., Fisher, N.I., 2002. Apatite as an indicator mineral for mineral exploration: trace-element compositions and their relationship to host rock type. J. Geochem. Explor. 76, 45–69.

Bhandari, N., Bhat, S.G., Lal, D., Rajagopalan, G., Tamhane, A.S.J., Venkatavaradan, V.S., 1971. Fission fragment tracks in apatite: recordable track lengths. Earth Planet. Sci. Lett. 13, 191–199.

Bigazzi, G., 1967. Length of fission tracks and age of muscovite samples. Earth Planet. Sci. Lett. 3, 434–438.

Bigazzi, G., 1981. The problem of the decay constant λ_F of ^{238}U. Nucl. Tracks 5, 35–44.

Bigazzi, G., Hadler, J.C., Iunes, P.J., Oddone, M., Paolo, S.R., Poupeau, G., 1990. On neutron dosimetry: comparison between different dosimeters: preliminary results. Nucl. Tracks 3, 217–221.

Boyce, J.W., Hodges, K.V., 2005. U and Th zoning in Cerro de Mercado (Durango, Mexico) fluorapatite: insights regarding the impact of recoil redistribution of radiogenic ^{4}He on (U–Th)/He thermochronology. Chem. Geol. 219, 261–274.

Carlson, W.D., Donelick, R.A., Ketcham, R.A., 1999. Variability of apatite fission-track annealing kinetics: I. Experimental results. Am. Mineral. 84, 1213–1223.

Chew, D.M., Donelick, R.A., 2012. Combined apatite fission track and U–Pb dating by LA-ICP-MS and its application in apatite provenance analysis. Mineralogical Association of Canada Short Course 42, 219–247.

Chew, D.M., Petrus, J.A., Kamber, B.S., 2014. U–Pb LA-ICPMS dating using accessory mineral standards with variable common Pb. Chem. Geol. 363, 185–199.

Chew, D.M., Sylvester, P.J., Tubrett, M.N., 2011. U–Pb and Th–Pb dating of apatite by LA-ICPMS. Chem. Geol. 280, 200–216.

Cochrane, R., Spikings, R.A., Chew, D.M., Wotzlaw, J.-F., Chiaradia, M., Tyrrell, S., Schaltegger, U., Van der Lelij, R., 2014. High temperature (>350°C) thermochronology and mechanisms of Pb loss in apatite. Geochim. Cosmochim. Acta 127, 39–56.

Corona-Esquivel, R., Tapia-Zúñiga, C., Henríquez, F., Tritlla, J., Morales-Isunza, A., Levresse, G., Pérez-Flores, E., 2009. Geology and mineralization of the Cerro de Mercado iron deposit, Durango. In: Clark, K.F., Salas-Pizá, G.A, Cubillas-Estrada, R. (Editors), Economic Geology of Mexico, 2nd edition, 529–535 (in Spanish).

Corona-Esquivel, R., Tritlla, J., Levresse, G., Henríquez, F., 2007. Presence of two Phanerozoic IOCG belts in México: geological framework and general characteristics. In: Andrew, C.J et al. (Editors), Proceedings of the Ninth Biennial Meeting of the Society for Geology Applied to Mineral Deposits Dublin, Ireland 20th-23rd August 2007, 1343–1346.

Cowan, G.A., Adler, H.H., 1976. The variability of the natural abundance of ^{235}U. Geochim. Cosmochim. Acta 40, 1487–1490.

Cox, S.E., Farley, K.A., Cherniak, D.J., 2015. Direct measurement of neon production rates by (α,n) reactions in minerals. Geochim. Cosmochim. Acta 148, 130–144.

Crowley, K.D., 1985. Thermal significance of fission-track length distributions. Nucl. Tracks Rad. Meas. 10, 311–322.

Crowley, K.D., 1993. LENMODEL: a forward model for calculating length distributions and fission-track ages in apatite. Comput. Geosci. 19, 619–626.

Curvo, E.A.C., Jonckheere, R., Guedes, S., Iunes, P.J., Tello, C.A., Hadler, J.C., Unterricker, S., Ratschbacher, L., 2013. A comparison between neutron-fluence measurements using metal-activation monitors and standard glasses calibrated via thin uranium-fission monitors and via ηq method. Radiat. Meas. 53–54, 38–44.

Danhara, T., Iwano, H., 2013. A review on the present state of the absolute calibration for zircon fission track geochronometry. Isl. Arc 22, 264–279.

Danišík, M., Sachsenhofer, R.F., Privalov, V.A., Panova, E.A., Frisch, W., Spiegel, C., 2008. Low-temperature thermal evolution of the Azov Massif (Ukrainian Shield — Ukraine) — implications for interpreting (U–Th)/He and fission track ages from cratons. Tectonophysics 456, 171–179.

Danišík, M., Štěpančíková, P., Evans, N.J., 2012. Constraining long-term denudation and faulting history in intraplate regions by multisystem thermochronology: an example of the Sudetic Marginal Fault (Bohemian Massif, Central Europe). Tectonics 31, TC2003. http://dx.doi.org/10.1029/2011TC003012.

De Corte, F., Van den haute, P., Dewispelaere, A., Jonckheere, R., 1991. Calibration of the fission track dating method: is Cu useful as an absolute thermal neutron fluence monitor? Chem. Geol. (Isot. Geosci. Sect.) 86, 187–194.

De Corte, F., Van den, P., Bellemans, F., 1995. The use of uranium doped glasses in fission-track dating. Radiat. Meas. 25, 511–516.

De Grave, J., Van den haute, P., 2002. Denudation and cooling of the Lake Teletskoye region in the Altai Mountains (South Siberia) as revealed by apatite fission-track thermochronology. Tectonophysics 349, 145–159.

Donelick, R.A., 1991. Crystallographic orientation dependence of mean etchable fission track length in apatite: an empirical model and experimental observations. Am. Mineral. 76, 83–91.

Donelick, R.A., Ketcham, R.A., Carlson, W.D., 1999. Variability of apatite fission-track annealing kinetics: II. Crystallographic orientation effects. Am. Mineral. 84, 1224–1234.

Donelick, R.A., Roden, M.K., Moers, J.D., Carpenter, B.S., Miller, D.S., 1990. Etchable length reduction of induced fission tracks in apatite at room temperature, (~23°C): crystallographic orientation effects and "initial" mean lengths. Nucl. Tracks *Radiat.* Meas. 17, 261–265.

Duddy, I.R., Green, P.F., Laslett, G.M., 1988. Thermal annealing of fission tracks in apatite. 3. Variable temperature behaviour. Chem. Geol. (Isot. Geosci. Sect.) 73, 25–38.

Eikenberg, J., Signera, P., Wieler, R., 1993. U–Xe, U–Kr, and U–Pb systematics for dating uranium minerals and investigations of the production of nucleogenic neon and argon. Geochim. Cosmochim. Acta 57, 1053–1069.

Enkelmann, E., Jonckheere, R., 2003. Correction factors for systematic errors related to the track counts in fission-track dating with the external detector method. Radiat. Meas. 36, 351–356.

Enkelmann, E., Jonckheere, R., Ratschbacher, L., 2005a. Absolute measurements of the uranium concentration in thick samples using external fission-track detectors. Nucl. Inst. Methods Phys. Res. B 229, 489–498.

Enkelmann, E., Jonckheere, R., Wauschkuhn, B., 2005b. Independent fission-track ages (ϕ-ages) of proposed and accepted apatite age standards and a comparison of ϕ-, Z-, ζ- and ζ_0-ages: implications for method calibration. Chem. Geol. 222, 232–248.

Enkelmann, E., Ratschbacher, L., Jonckheere, R., Nestler, R., Fleischer, M., Gloaguen, R., Hacker, B., Zhang, Y.Q., Ma, Y.S., 2006. Cenozoic exhumation and deformation of northeastern Tibet and the Qinling. Is Tibetan lower crustal flow diverging around the Sichuan Basin? Geol. Soc. Am. Bull. 118, 651–671.

Evans, N.J., Byrne, J.P., Keegan, J.T., Dotter, L.E., 2005. Use of ICP-MS for the determination of uranium and thorium in (U–Th)/He thermochronology. J. Anal. Chem. 60, 1300–1307.

Farley, K.A., 2000. Helium diffusion from apatite: general behavior as illustrated by Durango fluorapatite. J. Geophys. Res. 105, 2903–2914.

Farley, K.A., 2002. (U–Th)/He dating: techniques, calibrations, and applications. Rev. Mineral. Geochem. 47, 819–844.

Fleischer, R.L., Price, P.B., Walker, R.M., 1975. Nuclear Tracks in Solids. University of California Press, Berkeley, Principles and applications 604 pp.

Foeken, J.P.T., Stuart, F.M., Dobson, K.J., Persano, C., Vilbert, D., 2006. A diode laser system for heating minerals for (U–Th)/He chronometry. Geochem. Geophys. Geosyst. 7, 1–9.

Foshag, W.F., 1929. Mineralogy and geology of Cerro de Mercado, Durango, Mexico. Proceedings of the U.S. National Museum **74** 1–27 + 4 plates.

Galbraith, R.F., 1981.On statistical models for fission track counts. Math. Geol. **13**, 471–483.

Gautheron, C.E., Tassan-Got, L., Farley, K.A., 2006. (U–Th)/Ne chronometry. Earth Planet. Sci. Lett. 243, 520–535.

Gleadow, A.J.W., 1981. Fission track dating methods: what are the real alternatives? Nucl. Tracks 5, 3–14.

Gleadow, A.J.W., Duddy, I.R., 1981. A natural long-term track annealing experiment for apatite. Nucl. Tracks 5, 169–174.

Gleadow, A.J.W., Duddy, I.R., Green, P.F., Lovering, J.F., 1986. Confined fission track lengths in apatite: a diagnostic tool for thermal history analysis. Contrib. Mineral. Petrol. 94, 405–415.

Gleadow, A.J.W., Duddy, I.R., Lovering, J.F., 1983. Fission track analysis: a new tool for the evaluation of thermal histories and hydrocarbon potential. Australian Petroleum Exploration Association Journal 23, 93–102.

Gleadow, A., Harrison, M., Kohn, B., Lugo-Zazueta, R., Phillips, D., 2015. The Fish Canyon Tuff: a new look at an old low-temperature thermochronology standard. Earth Planet. Sci. Lett. 424, 95–108.

Goldoff, B., Webster, J.D., Harlov, D.E., 2012. Characterization of fluor-chlorapatites by electron probe microanalysis with a focus on time-dependent intensity variation of halogens. Am. Mineral. 97, 1103–1115.

Gong, G., Zhou, J., Sun, W., Xu, H., Yang, K., 2013. A novel mass spectrometry system for helium-4 measurement. J. Earth Sci. 24, 663–666.

Green, P.F., 1981. "Track-in-track" length measurements in annealed apatites. Nucl. Tracks 5, 121–128.

Green, P.F., 1985. Comparison of zeta calibration baselines for fission-track dating of apatite, zircon and sphene. Chem. Geol. (Isot. Geosci. Sect.) 58, 1–22.

Green, P.F., 1988. The relationship between track shortening and fission track age reduction in apatite: combined influences of inherent instability, annealing anisotropy, length bias and system calibration. Earth Planet. Sci. Lett. 89, 335–352.

Green, P.F., Duddy, I.R., Gleadow, A.J.W., Tingate, P.R., Laslett, G.M., 1986. Thermal annealing of fission tracks in apatite. 1. A qualitative description. Chem. Geol. (Isot. Geosci. Sect.) 59, 237–253.

Green, P.F., Duddy, I.R., Laslett, G.M., Hegarty, K.A., Gleadow, A.J.W., Lovering, J.F., 1989. Thermal annealing of fission tracks in apatite. 4. Quantitative modelling techniques and extension to geological timescales. Chem. Geol. (Isot. Geosci. Sect.) 79, 155–182.

Grimmer, J.C., Jonckheere, R., Enkelmann, E., Ratschbacher, L., Hacker, B.R., Blythe, A., Wagner, G.A., Wu, Q., Liu, S., Dong, S., 2002. Cretaceous–Cenozoic history of the southern Tan-Lu fault zone: apatite fission-track and structural constraints from the Dabie Shan (eastern China). Tectonophysics 359, 225–253.

Guedes, S., Hadler, J.C., Iunes, P.J., Paulo, S.R., Zuñiga, A., 2000. The spontaneous fission decay constant of ^{238}U using SSNTD. J. Radioanal. Nucl. Chem. 245, 441–442.

Guedes, S., Hadler, J.C., Iunes, P., Tello Saenz, C.A., 2004. Kinetic model for the relationship between confined fission-track length shortening and fission-track age reduction in minerals. Nucl. Inst. Methods Phys. Res. B 217, 627–636.

Guedes, S., Hadler, J.C., Sarkis, J.E.S., Oliveira, K.M.G., Kakazu, M.H., Iunes, P.J., Saiki, M., Tello, C.A., Paulo, S.R., 2003. Spontaneous-fission decay constant of U-238 measured by nuclear track techniques without neutron irradiation. J. Radioanal. Nucl. Chem. 258, 117–122.

Guedes, S., Jonckheere, R., Iunes, P.J., Hadler, J.C., 2008. Projected length distributions of fission tracks from U and Th thin film sources in muscovite. Nucl. Inst. Methods Phys. Res. B 266, 786–790.

Gunnell, Y., Gallagher, K., Carter, A., Widdowson, M., Hurford, A., 2003. Denudation history of the continental margin of western peninsular India since the early Mesozoic: reconciling apatite fission-track data with geomorphology. Earth Planet. Sci. Lett. 215, 187–201.

Hasebe, N., Barbarand, J., Jarvis, K., Carter, A., Hurford, A.J., 2004. Apatite fission-track chronometry using laser ablation ICP-MS. Chem. Geol. 207, 135–145.

Hasebe, N., Tamura, A., Arai, S., 2013. Zeta equivalent fission-track dating using LA-ICP-MS and examples with simultaneous U–Pb dating. Isl. Arc 22, 280–291.

Hoffmann, D.L., Paterson, B.A., Jonckheere, R., 2008. Measurements of the uranium concentration and distribution in a fossil equid tooth using fission tracks, TIMS and laser-ablation ICP-MS: implications for ESR dating. Radiat. Meas. 43, 5–13.

Hoke, G.D., Graber, N.R., Mescua, J.F., Giambiagi, L.B., Fitzgerald, P.G., Metcalf, J.R., 2015. Near pure surface uplift of the Argentine Frontal Cordillera: insights from (U–Th)/He thermochronometry and geomorphic analysis. In: Sepúlveda, S.A., Giambiagi, L.B., Moreiras, S.M., Pinto, L., Tunik, M., Hoke, G.D., Farías, M. (Editors), Geodynamic Processes in the Andes of Central Chile and Argentina. Geological Society of London Special Publications 399, 383–399.

Holden, N.E., 1989. Total and spontaneous fission half-lives for uranium, plutonium, americium and curium nuclides. Pure Appl. Chem. 61, 1483–1504.

Holden, N.E., 1999. Temperature dependence of the Westcott *g*-factor for neutron reactions in activation analysis (technical report). Pure Appl. Chem. 71, 2309–2315.

Holden, N.E., Hoffman, D.C., 2000. Spontaneous fission half-lives for ground state nuclides (technical report). Pure Appl. Chem. 72, 1525–1562.

Holden, N.E., Holden, K.A., 1989. Re-examination of 2200 meter/second cross-section experiments for neutron capture and fission standards. Pure Appl. Chem. 61, 1505–1510.

House, M.A., Farley, K.A., Kohn, B.P., 1999. An empirical test of helium diffusion in apatite: borehole data from the Otway basin, Australia. Earth Planet. Sci. Lett. 170, 463–474.

House, M.A., Farley, K.A., Stockli, D., 2000. Helium chronometry of apatite and titanite using Nd-YAG laser heating. Earth Planet. Sci. Lett. 183, 365–368.

Hurford, A.J., 1990a. International-Union-of-Geological-Sciences Subcommission on Geochronology recommendation for the standardization of fission-track dating calibration and data reporting. Nucl. Tracks Rad. Meas. 17, 233–236.

Hurford, A.J., 1990b. Standardization of fission-track dating calibration: recommendation by the Fission-Track Working Group of the I.U.G.S. Subcommission on Geochronology. Chem. Geol. (Isot. Geosci. Sect.) 80, 171–178.

Hurford, A.J., 1998. In: Van den haute, P., De Corte, F. (Eds.), Zeta: the ultimate solution to fission-track analysis calibration or just an interim measure?Kluwer Academic Publishers, Dordrecht, Advances in fission-track geochronology, pp. 19–32

Hurford, A.J., Green, P.F., 1981. A reappraisal of neutron dosimetry and uranium-238 λ_F values in fission-track dating. Nucl. Tracks 5, 53–61.

Hurford, A.J., Green, P.F., 1983. The zeta age calibration of fission-track dating. Isot. Geosci. 1, 285–317.

Iunes, P.J., Hadler, J.C., Bigazzi, G., Tello, C., Guedes, S., Paulo, S.R., 2002. Durango apatite fission-track dating using length-based age corrections and neutron fluence measurements by natural thorium thin films and natural U-doped glasses calibrated through natural uranium thin films. Chem. Geol. 187, 201–211.

Iwano, H., Danhara, T., 1998. In: Van den haute, P., De Corte, F. (Eds.), A re-investigation of the geometry factors for fission-track dating of apatite, sphene and zircon. Kluwer Academic Publishers, Dordrecht, Advances in fission-track geochronology, pp. 47–66.

Iwano, H., Kasuya, M., Danhara, T., Yamashita, T., Tagami, T., 1993. Track counting efficiency and unetchable track range in apatite. Nucl. Tracks Rad. Meas. 21, 513–517.

Iwano, H., Kasuya, M., Yamashita, T., Danhara, T., 1992. One-to-one correlation of fission tracks between zircon and mica detectors. Nucl. Tracks Rad. Meas. 20, 341–347.

Jaffey, A.H., Flynn, K.F., Glendenin, L.E., Bentley, W.C., Essling, A.M., 1971. Precision measurements of the half-lives and specific activities of 235 U and 238 U. Phys. Rev. C4, 1889–1906.

Jaskierowicz, G., Dunlop, A., Jonckheere, R., 2004. Track formation in fluorapatite irradiated with energetic cluster ions. Nucl. Inst. Methods Phys. Res. B 222, 213–227.

Johnstone, S., Hourigan, J., Gallagher, C., 2013. LA-ICP-MS depth profile analysis of apatite: protocol and implications for (U–Th)/He thermochronometry. Geochim. Cosmochim. Acta 109, 143–161.

Jonckheere, R., 1995. Absolute age determinations of apatite based on uranium fission tracks: a methodical investigation Ph.D. Thesis, Universiteit Gent, 504 pp. (in Flemish).

Jonckheere, R., 2003a. On methodical problems in deriving geological temperature and time from fission-track measurements in apatite. Radiat. Meas. 36, 43–55.

Jonckheere, R., 2003b. On the ratio of induced fission-track densities in a mineral and a co-irradiated muscovite external detector with reference to fission-track dating of minerals. Chem. Geol. 200, 41–58.

Jonckheere, R., Mars, M., Van den haute, P., Rebetez, M., Chambaudet, A., 1993. The apatite from Durango, Mexico: analysis of a standard mineral for fission-track dating. Chem. Geol. 103, 141–154 (in French).

Jonckheere, R., Enkelmann, E., Min, M., Trautmann, C., Ratschbacher, L., 2007. Confined fission tracks in ion-irradiated and step-etched prismatic sections of Durango apatite. Chem. Geol. 242, 202–217.

Jonckheere, R., Van den haute, P., 1996. Observations on the geometry of etched fission tracks in apatite: implications for models of track revelation. Am. Mineral. 81, 1476–1493.

Jonckheere, R., Van den haute, P., 1998. On the frequency distributions per unit area of the dimensions of fission tracks revealed in an internal and external mineral surface and in the surface of an external detector. Radiat. Meas. 29, 135–143.

Jonckheere, R., Van den haute, P., 1999. On the frequency distributions per unit area of the projected and etchable lengths of surface-intersecting fission tracks: influences of track revelation, observation and measurement. Radiat. Meas. 30, 155–179.

Jonckheere, R., Van den haute, P., 2002. On the efficiency of fission-track counts in an internal and external apatite surface and in a muscovite external detector. Radiat. Meas. 35, 29–40.

Jones, S.M., Dokka, R.K., 1990. Modeling fission track annealing in apatite: an assessment of uncertainties. Nucl. Tracks Rad. Meas. 17, 255–260.

Ketcham, R.A., 2005. Forward and inverse modeling of low-temperature thermochronometry data. Rev. Mineral. Geochem. 58, 275–314.

Ketcham, R.A., Carter, A., Donelick, R.A., Barbarand, J., Hurford, A.J., 2007. Improved measurement of fission-track annealing in apatite using *c*-axis projection. Am. Mineral. 92, 789–798.

Ketcham, R.A., Carter, A., Hurford, A.J., 2015. Inter-laboratory comparison of fission track confined length and etch figure measurements in apatite. Am. Mineral. 100, 1452–1468.

Ketcham, R.A., Donelick, R.A., Balestrieri, M.L., Zattin, M., 2009. Reproducibility of apatite fission-track length data and thermal history reconstruction. Earth Planet. Sci. Lett. 284, 504–515.

Ketcham, R.A., Donelick, R.A., Donelick, M.B., 2000. AFTSolve: a program for multi-kinetic modeling of apatite fission-track data. Geol. Mater. Res. 2, 1–32.

Kimura, J.-I., Danhara, T., Iwano, H., 2000. A preliminary report on trace element determinations in zircon and apatite crystals using excimer laser ablation – inductively coupled plasma mass spectrometry (ExLA-ICPMS). Fission Track Newsletter 13, 11–20.

Kohn, B.P., Gleadow, A.J.W., Brown, R.W., Gallagher, K., O'Sullivan, P.B., Foster, D.A., 2002. Shaping the Australian crust over the last 300 million years: insights from fission track thermotectonic imaging and denudation studies of key terranes. Aust. J. Earth Sci. 49, 697–717.

Kohn, B.P., Gleadow, A.J.W., Brown, R.W., Gallagher, K., Lorencak, M., Noble, W.P., 2005. Visualising thermotectonic and denudation histories using apatite fission track thermochronology. In: Reiners, P.W., Ehlers, T.A. (Eds.), Low Temperature Thermochronology: Techniques, Interpretations, and Applications. Rev. Mineral. Geochem. 58, pp. 527–565.

Kraml, M., Pik, R., Rahn, M., Selbekk, R., Carignan, J., Keller, J., 2006. A new multi-mineral age reference material for $^{40}Ar/^{39}Ar$, (U–Th)/He and fission track dating methods: the Limberg t3 tuff. Geostand. Geoanal. Res. 30, 73–86.

Lang, M., Devanathan, R., Toulemonde, M., Trautmann, C., 2015. Advances in understanding of swift heavy-ion tracks in complex ceramics. Curr. Opinion Solid State Mater. Sci. 19, 39–48.

Laslett, G.M., Gleadow, A.J.W., Duddy, I.R., 1984. The relationship between fission track length and track density in apatite. Nucl. Tracks 9, 29–38.

Laslett, G.M., Green, P.F., Duddy, I.R., Gleadow, A.J.W., 1987. Thermal annealing of fission tracks in apatite. 2. A quantitative analysis. Chem. Geol. (Isot. Geosci. Sect.) 65, 1–13.

Legrain, N., Stüwe, K., Wölfler, A., 2014. Incised relict landscapes in the eastern Alps. Geomorphology 221, 124–138.

Li, W., Kluth, P., Schauries, D., Rodriguez, M.D., Lang, M., Zhang, F., Zdorovets, M., Trautmann, C., Ewing, R.C., 2014. Effect of orientation on ion track formation in apatite and zircon. Am. Mineral. 99, 1127–1132.

Li, Q.-L., Li, X.-H., Wu, F.-Y., Yin, Q.-Z., Ye, H.-M., Liu, Y., Tang, G.-Q., Zhang, C.-L., 2012. In-situ SIMS U–Pb dating of Phanerozoic apatite with low U and high common Pb. Gondwana Res. 21, 745–756.

Lutz, T.M., Omar, G., 1991. An inverse method of modeling thermal histories from apatite fission-track data. Earth Planet. Sci. Lett. 104, 181–195.

Lyons, J.I., 1988. Volcanogenic iron oxide deposits, Cerro de Mercado and vicinity, Durango, Mexico. Econ. Geol. 83, 1886–1906.

Mahéo, G., Gautheron, C., Leloup, P.-H., Fox, M., Tassant-Got, L., Douville, E., 2013. Neogene exhumation history of the Bergell massif (southeast Central Alps). Terra Nova 25, 110–118.

Marks, M.A.W., Wenzel, T., Whitehouse, M.J., Loose, M., Zack, T., Barth, M., Worgard, L., Krasz, V., Eby, G.N., Stosnach, H., Markl, G., 2012. The volatile inventory (F, Cl, Br, S, C) of magmatic apatite: an integrated analytical approach. Chem. Geol. 291, 241–255.

McConnel, D., 1973. Apatite. Its crystal chemistry, mineralogy, utilization and geologic and biologic occurrences. In: Frechette, V.D., Kirsch, H., Sand, L.B., Trojer, F. (Eds.), Applied Mineralogy 5. Springer Verlag, Wien 111 pp.

McCubbin, F.M., Steele, A., Hauri, E.H., Nekvasil, H., Yamashita, S., Hemley, R.J., 2010. Nominally hydrous magmatism on the Moon. Proc. Natl. Acad. Sci. U. S. A. 107, 11223–11228.

McDowell, F.W., Keizer, R.P., 1977. Timing of the mid-Tertiary volcanism in the Sierra Madre Occidental between Durango City and Mazatlán, Mexico. Geol. Soc. Am. Bull. 88, 1479–1487.

McDowell, F.W., McIntosh, W.C., Farley, K.A., 2005. A precise ^{40}Ar-^{39}Ar reference age for the Durango apatite (U–Th)/He and fission-track dating standard. Chem. Geol. 214, 249–263.

Min, K., Reiners, P.W., Wolff, J.A., Mundil, R., Winters, R.L., 2006. (U–Th)/He dating of volcanic phenocrysts with high-U–Th inclusions, Jemez Volcanic Field, New Mexico. Chem. Geol. 227, 223–235.

Miro, S., Grebille, D., Chateigner, D., Pelloquin, D., Stoquert, J.-P., Grob, J.-J., Costantini, J.-M., Studer, F., 2005. X-ray diffraction study of damage induced by swift heavy ion irradiation in fluorapatite. Nucl. Inst. Methods Phys. Res. B 227, 306–318.

Moens, L., 1981. The k_0-comparator method as a new standardization technique in in reactor-neutron-activation analysis Ph.D. Thesis, Universiteit Gent, 354 pp. (in Flemish).

Morishita, T., Hattori, K.H., Terada, K., Matsumoto, T., Yamamoto, K., Takebe, M., Ishida, Y., Tamura, A., Arai, S., 2008. Geochemistry of apatite-rich layers in the Finero phlogopite-peridotite massif (Italian Western Alps) and ion microprobe dating of apatite. Chem. Geol. 251, 99–111.

Naeser, C.W., Crowley, K.D., McPherson, B.J., Cameron, M., 1989. The relationship between fission-track length and fission-track density in apatite. Geol. Soc. Am. Abstr. Programs 21, A241–A242.

Naeser, C.W., Fleischer, R.L., 1975. The age of the apatite at Cerro de Mercado, Mexico: a problem for fission track annealing corrections. Geophys. Res. Lett. 2, 67–70.

Nagpaul, K.K., Mehta, P.P., Gupta, M.L., 1974. Fission track ages of cogenetic minerals of the Nellore mica belt of India. Pure Appl. Geophys. 112, 140–148.

Op de Beeck, J., 1976. Description and Structure of the Programs GELIAN and MULTIP. Universiteit Gent, International Reports of the Institute for Nuclear Sciences 61 pp.

Patiño Douce, A.E., Roden, M.F., Chaumba, J., Fleisher, C., Yogodzinski, G., 2011. Compositional variability of terrestrial mantle apatites, thermodynamic modeling of apatite volatile contents, and the halogen and water budgets of planetary mantles. Chem. Geol. 288, 14–31.
Paul, T.A., Fitzgerald, P.G., 1992. Transmission electron microscopic investigation of fission tracks in fluorapatite. Am. Mineral. 77, 336–344.
Pellas, P., Perron, C., 1984. Track formation models: a short review. Nucl. Instrum. Methods 31, 387–393.
Piotraschke, R., Cashman, S.M., Furlong, K.P., Kamp, P.J.J., Danišík, M., Xu, G., 2015. Unroofing the Klamaths — blame it on Siletzia? Lithosphere 7, 427–440.
Price, P.B., Walker, R.M., 1963. Fossil tracks of charged particles in mica and the age of minerals. J. Geophys. Res. 68, 4847–4862.
Ravenhurst, C.E., Roden-Tice, M.K., Miller, D.S., 2003. Thermal annealing of fission tracks in fluorapatite, chlorapatite, manganoapatite, and Durango apatite: experimental results. Can. J. Earth Sci. 40, 995–1007.
Reiners, P.W., Nicolescu, S., 2006. Measurement of parent nuclides for (U–Th)/He chronometry by solution sector ICP-MS. Arizona Radiogenic Helium Dating Laboratory (ARDHL) Report 1, 1–33.
Roeder, P.L., MacArthur, D., Ma, X.-P., Palmer, G.R., 1987. Cathodoluminescence and microprobe study of rare-earth elements in apatite. Am. Mineral. 72, 801–811.
Rogers, P.S.Z., Duffy, C.J., Benjamin, T.M., Maggiore, C.J., 1984. Geochemical applications of nuclear microprobes. Nucl. Inst. Methods Phys. Res. B 3, 671–676.
Rønsbo, J.G., 1989. Coupled substitutions involving REEs and Na and Si in apatites in alkaline rocks from the Ilimaussaq intrusion, South Greenland, and the petrological implications. Am. Mineral. 74, 896–901.
Schauries, D., Afra, B., Bierschenk, T., Lang, M., Rodriguez, M.D., Trautmann, C., Li, W., Ewing, R.C., Kluth, P., 2014. The shape of ion tracks in natural apatite. Nucl. Inst. Methods Phys. Res. B 326, 117–120.
Schmidt, J.S., Lelarge, M.L.M.V., Conceicao, R.V., Balzaretti, N.M., 2014. Experimental evidence regarding the pressure dependence of fission track annealing in apatite. Earth Planet. Sci. Lett. 390, 1–7.
Shan, J., Min, K., Nouiri, A., 2013. Thermal effects of scanning electron microscopy on He diffusion in apatite: implications for (U–Th)/He dating. Chem. Geol. 345, 113–118.
Soares, C.J., Guedes, S., Hadler, J.C., Mertz-Kraus, R., Zack, T., Iunes, P.J., 2014. Novel calibration for LA-ICP-MS-based fission-track thermochronology. Phys. Chem. Miner. 41, 65–73.
Soares, C.J., Guedes, S., Tello, C.A., Lixandrão Filho, A.L., Osório, A.M., Alencar, I., Dias, A.N.C., Hadler, J., 2013. Further investigation of the initial fission-track length and geometry factor in apatite fission-track thermochronology. Am. Mineral. 98, 1381–1392.
Solé, J., Pi, T., 2005. An empirical calibration for ^{4}He quantification in minerals and rocks by laser fusion and noble gas mass spectrometry using Cerro de Mercado (Durango, Mexico) fluorapatite as a standard. Anal. Chim. Acta 535, 325–330.
Spiegel, C., Kohn, B., Belton, D., Berner, Z., Gleadow, A., 2009. Apatite (U–Th–Sm)/He thermochronology of rapidly cooled samples: the effect of He implantation. Earth Planet. Sci. Lett. 285, 105–114.
Steiger, R.H., Jäger, E., 1977. Subcommission on geochronology: convention on the use of decay constants in geo- and cosmochronology. Earth Planet. Sci. Lett. 36, 359–362.
Stock, M.J., Humphreys, M.C.S., Smith, V.C., Johnson, R.D., Pyle, D.M., Facility, E.I.M., 2015. New constraints on electron-beam induced halogen migration in apatite. Am. Mineral. 100, 281–293.
Storzer, D., Poupeau, G., 1973. Plateau ages of minerals and glasses with the fission track method. C. R. Acad. Sci. D276, 137–139 (in French).
Suzuki, T., 2005. Detection efficiency of fission tracks in apatite related to mica external detectors by the spike irradiation technique. Radiat. Meas. 40 (528), 531.
Swanson, E.R., Keizer, R.P., Lyons, J.I., Clabaugh, S.E., 1978. Tertiary volcanism and caldera development near Durango City, Sierra Madre Occidental, Mexico. Geol. Soc. Am. Bull. 89, 1000–1012.
Tagami, T., Nishimura, S., 1992. Neutron dosimetry and fission-track age calibration: insights from intercalibration of uranium and thorium glass dosimeters. Chem. Geol. (Isot. Geosci. Sect.) 102, 277–296.
Tamer, M.T., 2012. The Lengths of Fossil and Induced Fission Tracks in Durango Apatite. Thesis, Technische Universität Bergakademie Freiberg, M.Sc 37 pp.
Tello, C.A., Palissari, R., Hadler, J.C., Iunes, P.J., Guedes, S., Curvo, E.A.C., Paulo, S.R., 2006. Annealing experiments on induced fission tracks in apatite: measurements of horizontal-confined track lengths and track densities in basal sections and randomly oriented grains. Am. Mineral. 91, 252–260.
Teiber, H., Marks, M.A.W., Arzamastsev, A.A., Wenzel, T., Markl, G., 2015. Compositional variation in apatite from various host rocks: clues with regards to source composition and crystallization conditions. Neues Jb. Mineral. Abh. 192, 151–167.
Thomson, S.N., Gehrels, G.E., Ruiz, J., 2012. Routine low-damage apatite U–Pb dating using laser ablation-multicollector-ICPMS. Geochem. Geophys. Geosyst. 13, 1–23.
Van den haute, P., Chambaudet, A., 1990. Results of an interlaboratory experiment for the 1988 fission track workshop on a putative apatite standard for internal calibration. Nucl. Tracks Rad. Meas. 17, 247–252.
Van den haute, P., De Corte, F., Jonckheere, R., Bellemans, F., 1998. In: Van den haute, P., De Corte, F. (Eds.), The parameters that govern the accuracy of fission-track age determinations: a reappraisal. Kluwer Academic Publishers, Dordrecht, Advances in fission-track geochronology, pp. 33–46.
Van den haute, P., Jonckheere, R., De Corte, F., 1988. Thermal neutron fluence determination for fission track dating with metal activation monitors: a reinvestigation. Chem. Geol. (Isot. Geosci. Sect.) 73, 233–244.
Verheijke, M.L., 1994. Relation between the Høgdahl convention and the modified Westcott formalism for (n, γ) reactions with a pure $(1/v_n)$ cross-section behaviour. J. Radioanal. Nucl. Chem. 183, 293–299.
Wagemans, C., Schillebeeckx, P., Deruytter, A.J., Barthélémy, R., 1988. Subthermal fission cross-section measurements for ^{233}U, ^{235}U and ^{239}Pu. Proceedings of the International Conference on Nuclear Data for Science and Technology, Mito, Japan, Saikon Publishers Tokyo, pp. 91–95.
Wagner, G.A., Van den haute, P., 1992. Solid Earth Sciences Library Vol. 6. Kluwer Academic Publishers, Dordrecht 285 pp.
Warnock, A.C., Zeitler, P.K., Wolf, R.A., Bergman, S.C., 1997. An evaluation of low-temperature apatite U–Th/He thermochronometry. Geochim. Cosmochim. Acta 61, 5371–5377.
Watt, S., Durrani, S.A., 1985. Thermal stability of fission tracks in apatite and sphene: using confined track length measurements. Nucl. Tracks 10, 349–357.
Watt, S., Green, P.F., Durrani, S.A., 1984. Studies of annealing anisotropy of fission tracks in mineral apatite using track-in-track, TINT, length measurements. Nucl. Tracks 8, 371–375.
Wauschkuhn, B., Jonckheere, R., Ratschbacher, L., 2015a. The KTB apatite fission-track profiles: building on a firm foundation? Geochim. Cosmochim. Acta 167, 27–62.
Wauschkuhn, B., Jonckheere, R., Ratschbacher, L., 2015b. Xe- and U-tracks in apatite and muscovite near the etching threshold. Nucl. Inst. Methods Phys. Res. B 343, 146–152.
Willett, S.D., 1997. Inverse modeling of annealing of fission tracks in apatite 1: a controlled random search method. Am. J. Sci. 297, 939–969.
Wolf, R.A., Farley, K.A., Silver, L.T., 1996. Helium diffusion and low-temperature thermochronometry of apatite. Geochim. Cosmochim. Acta 60, 4231–4240.
Yang, Y.-H., Wu, F.-Y., Yang, J.-H., Chew, D.M., Xie, L.-W., Chu, Z.-Y., Zhang, Y.-B., Huang, C., 2014. Sr and Nd isotopic compositions of apatite reference materials used in U–Th–Pb geochronology. Chem. Geol. 385, 35–55.
Yoshioka, T., Tsuruta, T., Iwano, H., Danhara, T., 2005. Spontaneous fission decay constant of ^{238}U determined by SSNTD method using CR-39 and DAP plates. Nucl. Inst. Methods Phys. Res. A 555, 386–395.
Young, E.J., Myers, A.T., Munson, E.L., Conklin, N.M., 1969. Mineralogy and geochemistry of fluorapatite from Cerro de Mercado, Durango, Mexico. U.S. Geological Survey Professional Paper 650, pp. 84–93.
Zeitler, P.K., Herczeg, A.L., McDougall, I., Honda, M., 1987. U–Th–He dating of apatite: a potential thermochronometer. Geochim. Cosmochim. Acta 51, 2865–2868.
Zeng, Q., Evans, N.J., McInnes, B.I.A., Batt, G.E., McCuaig, C.T., Bagas, L., Tohver, E., 2013. Geological and thermochronological studies of the Dashui gold deposit, West Qinling Orogen, Central China. Mineral. Deposita 48, 397–412.